J. Appl. Cryst. (1980). **13**, 318–337

International Union of Crystallography

Commission on Crystallographic Apparatus

Microdensitometer Project Report
I. Inter-Experimental Agreement

By S. ABRAHAMSSON, *Department of Structural Chemistry, Faculty of Medicine, University of Göteborg, S-403 33 Göteborg, Sweden*, P. KIERKEGAARD, *Department of Structural Chemistry, Arrhenius Laboratory, University of Stockholm, Fack, S-104 05 Stockholm, Sweden* and E. ANDERSSON, O. LINDQVIST, G. LUNDGREN and L. SJÖLIN, *Department of Inorganic Chemistry, Chalmers University of Technology and University of Göteborg, S-412 96 Göteborg, Sweden*

(*Received* 10 *September* 1979; *accepted* 2 *February* 1980)

Abstract

The aim of the Microdensitometer Project was to investigate the agreement between intensity measurements performed by different laboratories. Each of fifteen participants was provided with four precession films prepared from two different crystals of sodium tartrate dihydrate: two films (*A* and *B*) of different exposure times from a small crystal and two similar films (*C* and *D*) from a larger crystal. A total of 33000 measured intensities and, in addition, 17000 scaled intensities were submitted for analysis.

The inter-film factor between films *A* and *B* and *C* and *D* was timed to be 3·0 and the average values obtained from the different data sets were 2·90 and 3·00, respectively. The processing of these data sets included an analysis of the spread of intensities for symmetry-related reflections both within any one experiment and between experiments. In addition, a calculation using the analysis of variance technique has been made based on the weighted deviations of intensities from the set of mean values in order to locate errors from various sources. By using an R_{sym} value defined later in the text as

$$R_{sym} = \frac{\sum_{hk}\sum_{s}|I_{hk,s} - I_{hk}|}{\sum_{hk} sI_{hk}},$$

the internal consistency within each experiment was evaluated from the *mm* symmetry in the film plane. The values of R_{sym} were found to lie in the ranges 0·055–0·102 and 0·043–0·073 for the *A* and *C* films respectively. R_{sym} values obtained from the average data sets constructed from the participants' scaled data, *B* to *A* and *D* to *C*, were 0.057 and 0.050 respectively. R_{mut} values were obtained by scaling the data sets in pairs using the scaling procedure of Hamilton, Rollett & Sparks (1965). The R_{mut} value was then defined as

$$R_{mut} = \sum_{hk}|I_i - I_j| / \sum_{hk}|I_i + I_j|$$

for experiments *i* and *j*; the range of observed values varied between 0·047 and 0·266 for the scaled data sets *B* to *A*, and between 0·039 and 0·143 for the scaled data sets *D* to *C*. It is clearly demonstrated in this report that the statistical spread of the intensities from films with small spots (*A*,*B*) is greater than that from films with large spots (*C*,*D*). It is important to note that the upper limit of measured optical density for a relevant estimate of the optical density is dependent on the size of the reflection; an upper limit of optical density which has proved useful for large reflections may be too high for small reflections.

This investigation has shown that the use of large computers (as usually found in off-line processing) may give more consistent data due to the possibility of using more extensive program systems. The report also includes a comparison of different types of linearity corrections, *i. e.* the use of either parabolic scaling or numerical correction of each density value, showing that the latter procedure on average gives slighty better agreement. It is difficult to draw definite conclusions about the light-beam size within this investigation, since only two participants use a small raster size (50 × 50 μm) for the measurement of the *A* and *B* films. However, their results indicate an improvement when the raster size is lowered. A comparison between different types of microdensitometers could not be performed as 12 of the 15 participating laboratories used the same microdensitometer model and the remaining three were all different. The real distribution of the intensities has been used as a basis for the comparison of different ways of estimating $\sigma(I)$. None of the formulae currently used could fully account for the real statistical spread. Finally, it may be concluded that the average microdensitometer system within this project gives X-ray diffraction data at a high level of accuracy, comparable with the results of the previous diffractometer project [Abrahams, Hamilton & Mathieson (1970). *Acta Cryst.* A**26**, 1–18].

Introduction

In 1969 the International Union of Crystallography's Commission on Crystallographic Apparatus presented the results of the Single Crystal Intensity Measurement Project (Abrahams, Hamilton & Mathieson, 1970) whose goal had been to obtain a comprehensive picture of the accuracy of intensity measurements using diffractometers and diffractometer systems. During the 10th International Crystallographic Congress in Amsterdam in 1975, a similar project was suggested for microdensitometers, the results to be presented at the 11th Congress in Warsaw, 1978.

During September 1976 about 80 laboratories were invited to participate in the project. The 34 who expressed a willingness to contribute data to the project using their normal routine procedures were sent a questionnaire, two multiple precession films (*A*, *B*) and an intensity scale. Subsequently, they received a second film set (*C*, *D*), previously measured in a different laboratory. Each particip-

0021-8898/80/030318-20$01.00

ant was requested to submit a data set from each film, containing the Miller indices, *hkl*, the integrated intensity, *I*, the position of the reflection (*x*, *y*) in film coordinates along **a*** and **b***, respectively, and the standard deviation, $\sigma(I)$, based on the measured distribution of optical density. The submission of film coordinates, (*x*, *y*), and $\sigma(I)$ was optional. In addition, scaled data sets (*E* from films *A* and *B*, and *F* from films *C* and *D*), resulting from the user's normal scaling procedure, and, if possible, standard deviations for the averaged intensities were requested. After having received the first set, 18 laboratories reported that either the software (10) or the hardware (8) was not working satisfactorily. 15 laboratories submitted measurements from all films and completed the questionnaires.

Data from all participants were received by the end of March 1977. A preliminary analysis of the mutual and internal consistencies was performed and presented at an Open Commission Meeting during the Fourth European Crystallographic Meeting in Oxford, August 1977 (ECM-4), at which time the Commission on Crystallographic Apparatus invited other laboratories to participate. However, no other laboratories expressed any interest. The participants in the project are listed alphabetically in Table 1, but this list is not correlated in any way with the data in the subsequent tables of the report.

So that as many as possible could participate in the project, precession geometry was chosen. In order to obtain good quality films, the crystal had to be stable during exposure. For consistency analysis *mm* symmetry is desirable in the plane of the film. Furthermore, the axes in the plane of the film must be long enough to give a sufficient number of reflections in each quadrant for statistical treatment. Absorption and other diffraction effects should be small and the specimen shape selected so as not to disturb the symmetry relations. The substance finally chosen for the project was sodium tartrate dihydrate, $C_4H_4Na_2O_6.2H_2O$, which crystallizes in $P2_12_12_1$ with $a = 11{\cdot}460\,(5)$, $b = 14{\cdot}670\,(5)$ and $c = 4{\cdot}959\,(3)$ Å (Ambady & Kartha, 1968). In the production of the films, the *c* axis was chosen as the precession axis, thus giving *hk*0 films.

Graphite-monochromated Mo $K\alpha$ radiation, a crystal-to-film distance of 60 mm and a precession angle of 24° gave a total of about 800 reflections per film. Film *A* (9 h exposure) and film *B* (3 h exposure) were obtained from a crystal of

Table. 1. *Participants in the IUCr Microdensitometer Project*

Buehner, M. & Metter, M.	Zentralbau Chemie, University of Würzburg, Federal Republic of Germany
Chirgadze, Y. N., Nikonov, S. V. & Kuzin, A. P.	Institute of Protein Research, Academy of Sciences of USSR, Moscow, USSR
Cohen, G., Navia, M. A. & Davies, D. R.	National Institutes of Health, Bethesda, MD, USA
Cygler, M.	Institute of Chemistry, University of Lódz, Novotki, Poland
Elder, M. & Machin, P.	SRC Microdensitometer Service, Warrington, England
Lindqvist, O., Olsson, G. & Sjölin, L.	Institute of Inorganic Chemistry, University of Göteborg, Göteborg, Sweden
Moffat, I. K., Siegel, B. M. & Szebenyi, D. M	Section of Biochemistry, Cornell University, Ithaca, NY, USA
Muirhead, H.	Dept of Biochemistry, University of Bristol, Bristol, England
Nyborg, J. & La Cour, T.	Institute of Chemistry, University of Aarhus, Aarhus, Denmark
Perlo, A. & Wyckoff, H. W.	Dept of Molecular Biophysics and Biochemistry, Yale Station, New Haven, USA
Reeke, G. N., Becker, J. W. & Edelman, G. M.	Lab. of Molecular and Developmental Biology, The Rockefeller University, NY, USA
Schoone, I. C.	Universiteit Utrecht, Utrecht, The Netherlands
Sherfinsky, I. S. & Rich, A.	Lab. of Molecular Structure, Cambridge, MA, USA
Starkey, J.	Dept of Geology, University of Western Ontario, Ontario, Canada
Werner, P. E.	Arrhenius Lab., University of Stockholm, Stockholm, Sweden

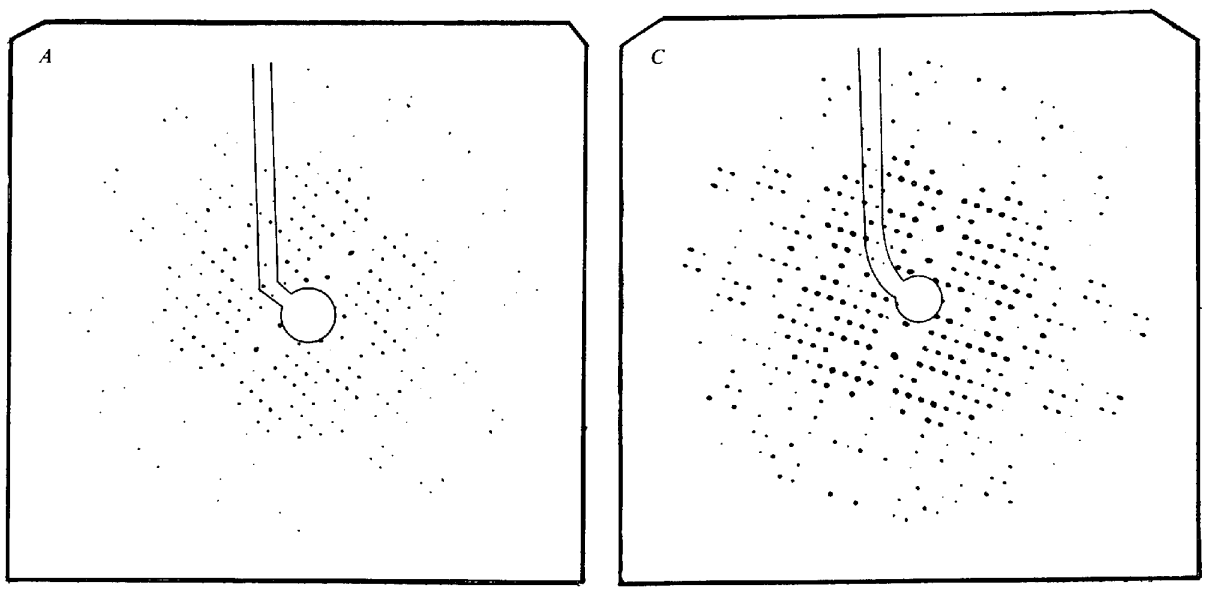

Fig. 1. *A* and *C* precession films used in the IUCr Microdensitometer Project, showing the amount of shielding due to the beam stopper.

dimensions 0·3 × 0·4 × 0·12 mm, while a crystal of dimensions 0·6 × 0·8 × 0·4 mm was used for the production of films *C* (1 ½ h exposure) and *D* (½ h exposure) (*cf.* Fig. 1). The reflection profiles are shown in Table 2. In addition, an intensity scale was prepared by timed exposure of the attenuated primary beam. Ilford Industrial G X-ray films from the same production batch were used and efforts were made to develop all films under uniform conditions. Accidental variations in intensity on the films ought to become apparent during the analysis, since, in general, each film set (both *A*/*B* and *C*/*D*) was sent to two different laboratories. No such variation has yet been detected. Since geometrical difficulties prevented the use of a flying beam stop, a normal beam stop was used, the arm of which partially or totally shielded some reflections. The amount of shielding on films *A* and *C* can be seen in Fig. 1.

A total of 35 reflections for the *A*/*B* films and 37 reflections for the *C*/*D* films, distributed mainly between two quadrants, have been rejected from each data set before analysis, although not always by the participants.

The present report deals with the inter-experimental agreement. Report II, which will be published subsequently, will be based on comparison of the film data with diffractometer data and on structure refinement using the submitted film intensities.

Experimental procedures

A summary of some general items of information obtained from the questionnaires is given in Tables 3 and 4. The data submitted by each of the participants has been assigned an identification number, which serves as a reference in the remainder of the report. Optronics P-1000 microdensitometers were used by 12 laboratories, while the other three used a Schnell photometer III, a Saab Mark II and a Syntex AD-1 microdensitometer. The computers used for the processing and evaluation work varied considerably. Five of the systems used an off-line computer, *i.e.* one which is not connected to the microdensitometer. In these cases magnetic tape was generally used for intermediate data storage. There were nine on-line systems, in which the evaluation of each integrated intensity took place immediately after reading the corresponding optical densities. One participant used a manual microdensitometer. As is seen from Table 3, the speed of the evaluation is usually a function of the core capacity of the computer.

Table 4 shows the choice of scanning area for the different films *A*/*B* and *C*/*D*. The method used to determine the orientation matrix is also indicated. Most laboratories perform a least-squares refinement using 4–24 manually indexed reflections.

There are three main methods which have been used in microdensitometry to correct for the non-linearity dependence of the intensity on the measured optical density: (1) parabolic scaling of a film pack; (2) direct biasing of the microdensitometer logarithmic amplifier circuit; (3) numerical correction of each density value based on previous calibration against an intensity scale.

The non-linearity compensation given in Table 4 divides the laboratories into two groups. Laboratories 11, 12, 13, 14 and 15 used the parabolic scaling procedure for the two successive films in each film pack (method 1). The other laboratories applied a non-linearity correction to each density measurement either from calibration charts or by some mathematical function obtained from measurements on a standard intensity scale (method 2). Scale factors and scaling

Table 2. *Print-out from a microdensitometer of a weak, medium and strong reflection*

σ is calculated according to the formula used by participant no. 6 (*cf.* Table 4).

(*a*) *A* film

19	19	20	21	21	21	22	19	19	20	19	19	22	20	20	21	20
20	19	22	20	22	21	19	22	23	20	20	22	19	20	18	20	22
21	20	22	21	21	22	20	21	22	20	20	21	21	20	20	21	19
24	19	20	19	22	21	21	22	21	22	20	21	20	18	19	22	23
20	22	19	19	19	22	21	22	22	22	20	22	19	21	20	19	21
21	20	22	19	21	22	25	25	24	23	21	21	20	20	19	20	18
21	20	19	22	21	22	22	26	26	23	21	19	19	20	20	19	20
22	21	19	20	20	22	20	22	23	25	22	22	21	22	19	19	20
19	21	20	19	20	21	23	20	24	20	18	20	19	20	19	19	21
21	20	19	20	21	20	20	19	20	18	19	20	21	22	19	20	22
20	22	19	19	22	20	20	22	20	22	21	20	20	20	20	19	21
21	21	18	20	19	20	20	22	20	20	19	21	23	24	20	21	21
20	21	19	21	20	20	20	19	20	21	20	20	20	20	21	19	19

$H=-5$ $K=-3$ $L=0$ INTENSITY = 48 $\sigma=23$

21	22	22	22	21	23	22	22	20	20	22	22	22	20	21	21	22
20	21	22	22	23	23	22	22	21	22	22	20	20	22	21	23	20
20	22	22	20	23	23	23	22	25	22	21	23	21	21	21	22	22
21	22	21	25	24	27	28	31	30	25	23	23	21	19	22	22	19
19	21	21	20	24	33	49	62	58	46	30	22	21	21	21	23	23
23	23	21	22	24	40	84	116	117	79	38	24	19	22	21	20	22
22	22	22	21	27	53	113	160	158	113	49	26	21	20	21	20	20
20	21	22	22	27	44	93	150	151	96	47	27	23	20	23	20	22
21	22	23	22	24	30	44	70	76	53	33	28	24	24	23	25	22
21	21	24	24	22	22	25	32	35	31	28	26	26	24	24	23	21
21	21	21	23	22	21	21	22	24	26	25	26	28	23	23	20	25
21	23	23	21	20	21	20	22	21	22	24	26	26	23	23	22	21
21	19	23	22	23	21	21	21	22	20	23	21	22	23	23	22	21

$H=0$ $K=-6$ $L=0$ INTENSITY = 1950 $\sigma=28$

23	23	25	23	24	23	22	23	24	26	27	29	27	25	26	23	23
23	22	23	23	24	24	22	26	26	26	32	31	29	27	24	22	22
22	23	23	24	26	24	26	27	31	35	41	40	33	28	24	23	27
24	22	24	23	26	26	26	33	39	46	49	47	40	31	23	25	22
23	22	24	25	28	34	46	56	59	59	62	56	37	28	25	23	25
25	26	24	27	44	89	135	144	128	109	73	52	38	25	24	22	22
24	23	23	26	47	140	186	189	184	172	106	50	32	24	24	22	22
24	24	24	26	41	106	204	206	204	199	162	57	28	26	22	22	22
24	22	23	25	32	59	146	215	214	211	187	71	26	24	23	22	22
22	22	24	24	28	41	69	132	213	213	155	61	29	23	23	24	21
22	24	23	24	31	37	51	53	60	64	52	36	26	24	23	24	23
22	22	22	24	30	36	36	38	32	30	29	27	24	26	23	25	22
22	23	22	24	29	38	30	30	27	27	25	27	26	23	24	22	22

$H=-4$ $K=0$ $L=0$ INTENSITY = 5625 $\sigma=25$

(*b*) *C* film

20	19	18	19	19	20	21	20	20	20	20	20	21	20	20	20	19
20	19	19	21	18	19	19	19	20	20	20	20	17	21	21	19	18
20	18	19	20	18	21	21	22	21	20	20	22	18	20	18	18	18
20	20	20	20	20	20	22	22	23	21	20	20	20	22	18	19	20
20	20	19	20	21	20	23	25	22	22	22	21	19	22	19	19	19
19	21	20	20	21	21	22	22	26	23	22	21	19	18	20	20	20
20	19	20	21	20	22	22	22	23	24	23	22	19	20	20	18	21
19	20	20	21	20	21	23	23	24	23	20	22	20	21	20	19	20
19	20	18	19	18	20	20	22	21	21	21	21	20	21	18	21	19
20	18	19	20	19	20	21	19	22	22	20	19	21	20	19	21	20
18	18	19	21	18	22	20	20	20	20	22	22	20	19	21	19	20
19	19	19	20	21	20	18	20	20	20	20	20	18	20	21	18	19
22	20	18	19	19	20	19	22	22	20	19	19	18	21	20	19	18

$H=-5$ $K=-3$ $L=0$ INTENSITY = 173 $\sigma=18$

19	19	20	18	21	20	20	20	19	21	18	19	23	21	23	20	19
16	21	20	20	22	23	25	26	23	20	22	22	21	19	20	20	18
22	23	21	22	26	27	32	34	32	30	25	25	21	20	20	20	19
19	20	21	26	32	37	46	52	48	51	39	32	26	21	20	19	20
20	20	21	26	36	46	58	70	72	68	60	51	36	24	23	21	19
20	21	23	27	41	57	79	88	91	92	82	67	49	31	23	22	22
19	19	23	28	45	62	80	94	102	104	98	80	57	37	25	20	18
21	18	20	26	38	54	74	95	102	104	97	91	60	36	26	22	22
20	21	20	24	32	42	62	77	92	93	95	79	54	35	24	21	22
18	19	22	23	28	32	40	57	71	76	74	58	41	28	25	22	21
19	21	20	20	23	25	27	35	47	50	44	37	28	24	24	24	21
18	19	18	21	22	20	21	26	24	26	27	25	24	23	21	20	22
22	21	21	19	19	20	22	20	21	23	23	22	20	20	20	19	23

$H=0$ $K=-6$ $L=0$ INTENSITY = 3277 $\sigma=29$

22	24	24	26	28	29	31	33	31	31	26	24	26	25	21	19	24
22	23	25	28	36	40	40	38	38	34	28	26	21	20	23	23	21
23	24	31	39	50	62	84	68	54	47	40	30	28	24	23	22	22
24	25	32	56	90	112	133	132	123	92	66	50	34	26	25	23	23
25	28	39	67	114	146	168	174	170	154	130	99	60	37	26	22	22
23	25	40	75	114	162	184	194	190	184	169	142	103	62	34	24	21
22	25	36	74	115	159	192	203	203	201	193	177	149	94	46	29	23
24	23	29	50	100	159	197	211	212	211	206	196	172	115	62	30	21
21	24	23	33	56	93	176	211	217	217	213	205	177	102	54	29	22
24	25	22	26	31	41	67	98	178	204	201	167	98	66	36	24	22
21	22	21	22	23	30	35	47	56	69	65	57	46	36	27	23	22
20	22	22	22	24	27	31	35	40	41	39	35	29	25	22	20	22
22	23	22	22	23	23	27	31	34	36	33	31	25	22	21	21	21

$H=-4$ $K=0$ $L=0$ INTENSITY = 10555 $\sigma=50$

agreement could only be investigated for the second group.

The variance of an integrated intensity has been evaluated in different ways. Seven laboratories did not report $\sigma(I)$ in their data sets. The statistical formulae used by the other eight laboratories are given in Table 4.

Estimation of the background comprises use of rectangles, frames, strips or boxes positioned outside the integration area. However, in most cases, the areas selected for background measurement lie as strips on two opposite sides of the reflection. In many systems the positioning and size of the area for background estimation can be selected *via* input instructions making the system flexible for different types of reciprocal lattice. The reflection positions were submitted by ten laboratories (*cf.* Table 4). This calculation is not normally included in the users' routine systems but was requested in order to detect errors due to the orientation matrix. However, the available (x, y) values were found to differ too much to be useful for statistical analyses in this project.

Preliminary treatment of the data

The data were submitted on punched cards or, in a few cases, on magnetic tape. All calculations within the project were performed on a DEC 10 computer. After storage of the submitted data on disc, the material was edited, and a few values with obvious errors were eliminated.

About 33000 individually measured intensities and, in addition, 17000 scaled intensities were stored as 86 data sets, in general six for each participant, as specified in Table 5. Table 6 shows the number of reflections contributed to the project by each participant. The *B* data set of participant No. 12 was damaged in transit and had to be totally rejected. Participant No. 10 submitted intensities only from films *C* and *D*.

As the user indications of supersaturated reflections or insignificant reflections varied from case to case and the absolute intensity scale also differed considerably between the experiments, a prescaling and editing program was written. The scale factors obtained between the different experiments varied from 0·24 to 2980.* One unit of intensity corresponds to about 250 photons, assuming that OD = 1 is the blackening obtained by 0·5 photon/μm^2 (Morimoto & Uyeda, 1963) using Ilford Industrial G film and Mo $K\alpha$ radiation.

The number of reflections submitted varies considerably (*cf.* Table 6), *e.g.* from 426 to 783 for the *A* film. This variation is due to different ways of defining a significance level. Some of the participants only submitted reflections which they considered significant, while others included all measurements. In a few cases it appeared that certain reflections had been rejected by the participants after inspection of their data sets.

For data sets which did not include standard deviations, $\sigma(I)$ values were estimated by comparison with the results from other laboratories after the data sets had been placed on a common scale. In the subsequent statistical analyses, only reflections with $I > 3\sigma(I)$ were considered significant. Due to the different ways in which $\sigma(I)$ was defined, the number of reflections used (Table 5, colums ii) varies from case to case. When comparing the precision of the different experiments in the following sections, these variations should be borne in mind.

Internal consistency

For each film the agreement between symmetry-related reflections was defined as

$$R_{sym} = \frac{\sum_{hk}\sum_{s}|I_{hk,s} - I_{hk}|}{\sum_{hk} s\, I_{hk}}, \qquad (1)$$

where s is the number of symmetry-related reflections ($s = 4$ for $h, k > 0$; $s = 2$ for $h = 0$ or $k = 0$), thus giving the degree of

* A complete list of the submitted intensities has been deposited with the British Library Lending Division as Supplementary Publication No. SUP 35089 (82 pp.). Copies may be obtained through The Executive Secretary, International Union of Crystallography, 5 Abbey Square, Chester CH1 2HU, England.

Table 3. *Microdensitometer systems*

Exp. no.	On-line/ off-line system	Program language	Core requirement (kbyte)	Speed of program (reflections/min)
1	On-line	Algol 6	24	35
2	Off-line	Fortran IV	200	260
3	Off-line	Fortran IV	246	240
4	On-line	Fortran IV	64	32
5	*	–	–	–
6	On-line	Fortran II assembler	32	30
7	On-line	Fortran IV assembler	220	40
8	Off-line	Fortran IV	116	70
9	On-line	Fortran macro	28	48
10	On-line	Fortran macro	24	70
11	On-line	Assembler	32	70
12	Off-line	Fortran II assembler	24	15
13	Off-line	Fortran IV	320	120
14	On-line	Fortran IV assembler	56	50
15	On-line	Assembler	16	15

* Manual microdensitometer.

Table 4. *Technical details*

Exp. no.	Scanning area of each reflection (mm)		How is the orientation of the film pattern established?	How are non-linearities in the OD measured and corrected for?	Delivered *xy* position on films?	The variance of each reflection is evaluated according to
	Film *A*, *B*	Film *C*, *D*				
1	0·65 × 0·75	1·05 × 1·15	Least-squares refinement	$D = D_m(1 - e^{-\alpha I})$	Yes	$\mathrm{Var}(I) = \mathrm{Var}(B)[N_i + N_i^2/N_b]$
2	1·1 × 1·1	1·05 × 1·15	Least-squares refinement	Calibration table	Yes	$\mathrm{Var}(I) = \Sigma(P_{OD} + B_{OD} - \mathrm{Tot}_{OD})^2(N_i/N_i)^2$
3	1·7 × 1·7	2·1 × 2·3	Least-squares refinement	$I_c = I_m + (I_m/19)^2$	Yes	$\mathrm{Var}(I) = \Sigma(P_{OD} + B_{OD} - \mathrm{Tot}_{OD})^2(N_i/N_i)^2$
4	1·2 × 1·2	1·2 × 1·2	Least-squares refinement	Three-degree polynomial	No	$\mathrm{Var}(I) = \Sigma(P_{OD} + B_{OD} - \mathrm{Tot}_{OD})^2(N_i/N_i)^2$
5	Not given	Not given	Least-squares refinement	Calibration curve	No	$\mathrm{Var}(I) = \mathrm{Var}(B)[N_i + N_i^2/N_b]$
6	0·6 × 0·6	1·0 × 1·0	Least-squares refinement	$I_c = I_m + (I_m/46)^3$	Yes	$\mathrm{Var}(I) = \mathrm{Var}(P) + (N_i/N_b)^2\mathrm{Var}(B)$
7	1·1 × 0·9	1·5 × 1·2	Least-squares refinement	$I_c = A + BI_m + CI_m^2 + DI_m^3$	Yes	$\mathrm{Var}(I) = \mathrm{Var}(P) + (N_i/N_b)^2\mathrm{Var}(B)$
8	0·8 × 0·8	0·8 × 0·8	Manual measurement	$I_c = A + BI_m + CI_m^2 + DI_m^3$	Yes	$\mathrm{Var}(I) = \Sigma P_{OD} + (N_i/N_b)^2\Sigma B_{OD}$
9	1·1 × 1·1	1·5 × 1·5	Least-squares refinement	$D = D_m(1 - e^{-\alpha I})$	No	$\mathrm{Var}(I) = \Sigma P_{OD} + (N_i/N_b)^2\Sigma B_{OD}$
10	1·1 × 1·1	1·9 × 1·3	Least-squares refinement	Four-degree polynomial	No	$\mathrm{Var}(I) = \Sigma P_{OD} + (N_i/N_b)^2\Sigma B_{OD}$
11	1·1 × 0·9	1·9 × 1·7	Automatic search	Parabolic scaling	Yes	$\mathrm{Var}(I) = \Sigma P_{OD} + (N_i/N_b)^2\Sigma B_{OD}$
12	1·1 × 0·9	1·9 × 1·7	Adjusted using 15 reflections	Parabolic scaling	Yes	$\mathrm{Var}(I) = \Sigma P_{OD} + (N_i/N_b)^2\Sigma B_{OD}$
13	1·1 × 1·1	1·1 × 1·1	Least-squares refinement	Parabolic scaling	No	From variations in R_{sym}
14	1·3 × 2·3	1·3 × 1·5	Least-squares refinement	Parabolic scaling	No	$\mathrm{Var}(I) = E[(\Sigma P_{OD})^2 + (N_i/N_b)^2(\Sigma B_{OD})^2]$
15	0·5 × 0·5	1·4 × 1·0	Least-squares refinement	Parabolic scaling	Yes	Statistically from repeated measurements

Table 5. *Naming of the different data sets*

Data obtained from	Data set name
Film *A*, small spots, long exposure time	*A*
Film *B*, small spots, short exposure time	*B*
Film *C*, large spots, long exposure time	*C*
Film *D*, large spots, short exposure time	*D*
Scaled data, *A* to *B*	*E*
Scaled data, *C* to *D*	*F*

Table 6. *A summary of the total number of intensities submitted* (*columns* i) *and the number of significant observations* (*columns* ii)

Exp.	Film *A*		Film *B*		Film *C*		Film *D*		Set *E*		Set *F*	
	i	ii	i	ii	i	ii	i	ii	i	ii	i	ii
1	587	273	236	142	614	448	275	260	580	270	611	443
2	426	317	362	218	552	472	441	316	421	309	543	456
3	552	268	562	179	589	416	566	287	533	260	582	411
4	720	368	720	237	719	470	720	323	720	365	719	465
5	492	442	345	313	489	488	367	360	474	440	486	486
6	783	362	788	237	822	481	823	332	774	355	813	330
7	691	344	704	229	708	486	712	367	687	311	702	455
8	653	544	669	602	487	467	645	310	652	522	589	446
9	722	287	722	186	720	370	720	231	720	263	719	330
10	–	–	–	–	717	478	718	319	–	–	715	465
11	556	287	317	191	662	449	453	310	575	291	651	426
12	660	385	–	–	550	444	439	297	663	381	543	426
13	520	327	221	167	565	463	185	185	345	339	360	354
14	671	336	704	243	677	435	706	343	611	330	643	431
15	575	353	576	205	590	507	583	452	570	330	575	503

Table 7. *Intervals used for analysis of agreement factors*

Range	Min.	Max.	OD (approx. max.) *A*/*B* set	OD (approx. max.) *C*/*D* set
1	0	200	0·49	0·38
2	200	400	0·59	0·47
3	400	700	0·85	0·54
4	700	1300	1·29	0·71
5	1300	2400	2·0	0·99
6	2400	3500	2·9	1·39
7	3500		> 3	> 1·50

internal consistency. The variation of R_{sym} with the intensity has been investigated using the intensity intervals listed in Table 7.

Tables 8 and 9 show the results from the *A* and *C* data sets respectively. Figs. 2–5 illustrate the R_{sym} distributions for all experiments. The number of reflections in each interval is also indicated. It is apparent that the films with smaller spots resulted in worse agreement between symmetry-related reflections. The statistical spread for the weak reflections is generally quite high. Some of the experiments show a slight increase in *R* for the strongest intensities (*cf.* Figs. 2–5), while in other experiments the *R* values fall off and converge towards a limiting value. The tendency to increase indicates systematic errors to be discussed later.

The user-scaled data sets (*E* and *F*) were also analysed in order to investigate differences in the R_{sym} distribution. The internal consistency of data sets *E* and *F* (Figs. 6 and 7) is closely related to that of data sets *A* and *C* (Figs. 2 and 4). By using Hamilton, Rollett & Sparks's (1965) scaling procedure (program *SCALE*), the *A* and *B*, and *C* and *D* data sets, respectively, have been scaled together to obtain film-factor values for each experiment.

Table 8. *R values from A-film data sets based on symmetry-related reflections*

R_{sym} values (all reflections) and R values from different intensity intervals.

Exp. no.	R_{sym}	R_1	R_2	R_3	R_4	R_5	R_6	R_7
1	0·102	0·174	0·111	0·101	0·081	0·074	–	–
2	0·080	0·095	0·111	0·094	0·071	0·069		–
3	0·063	0·088	0·088	0·080	0·064	0·048	*	–
4	0·065	0·147	0·112	0·098	0·076	0·043	*	–
5	0·073	0·163	0·118	0·120	0·077	0·040	*	–
6	0·055	0·126	0·093	0·078	0·053	0·044	*	–
7	0·076	0·112	0·107	0·099	0·085	0·056	*	–
8	0·104	0·213	0·215	0·159	0·090	0·056	*	–
9	0·058	–	0·128	0·103	0·095	0·077	0·055	0·032
10	–	–	–	–	–	–	–	–
11	0·078	0·119	0·112	0·093	0·086	0·050	*	–
12	0·063	0·119	0·109	0·089	0·060	0·042	*	–
13	0·065	0·090	0·073	0·070	0·062	0·048	*	–
14	0·098	0·173	0·133	0·102	0·089	0·053	*	–
15	0·070	0·101	0·093	0·092	0·053	0·070	*	–

* Non-significant number of reflections in the interval.

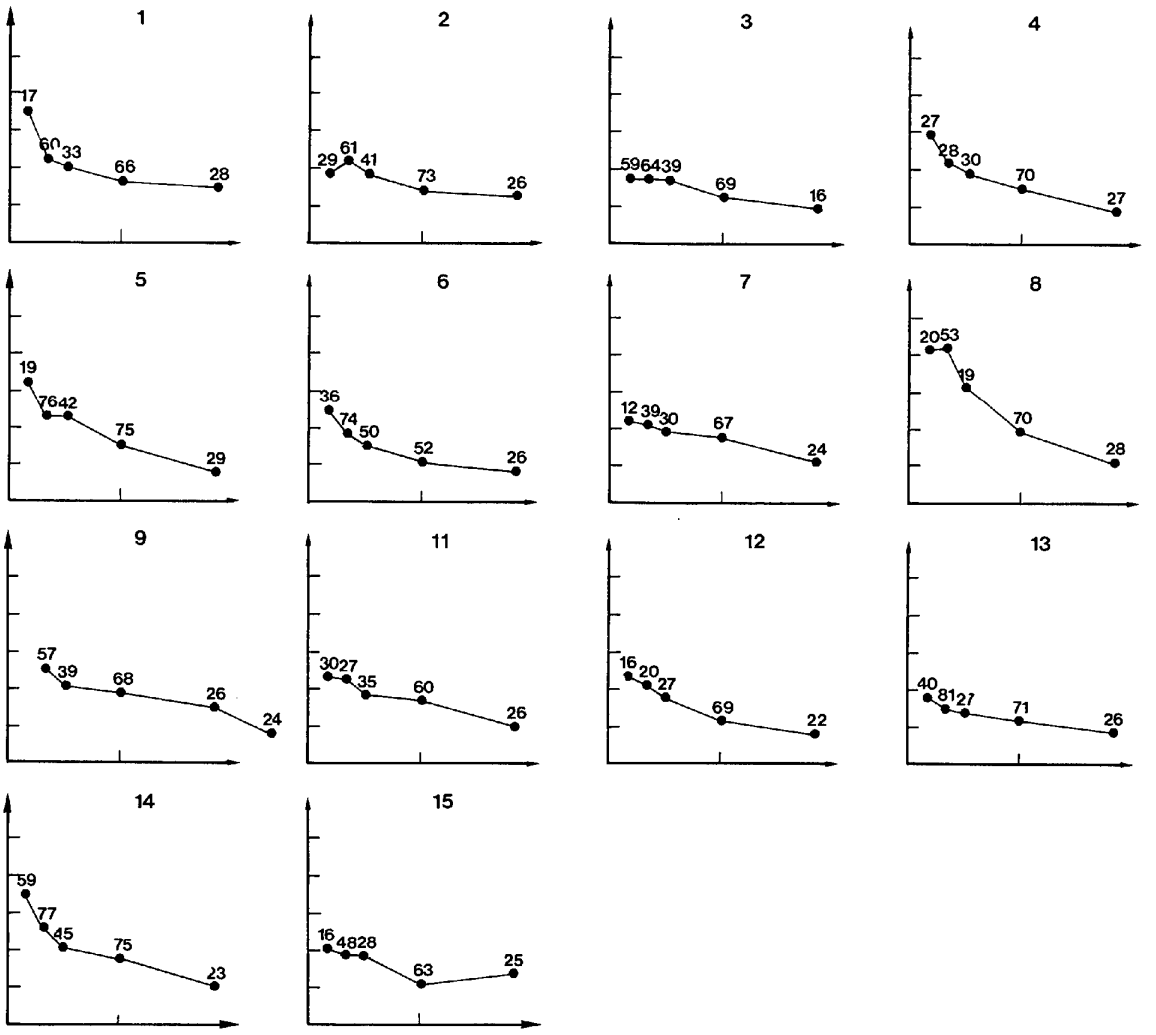

Fig. 2. R_{sym} values plotted against the intensity. All experiments from *A* film set.

Table 9. *R values from C-film data sets based on symmetry-related reflections*

R_{sym} values (all reflections) and R values from different intensity intervals.

Exp. no.	R_{sym}	R_1	R_2	R_3	R_4	R_5	R_6	R_7
1	0·073	0·157	0·109	0·087	0·071	0·054	0·071	*
2	0·066	0·099	0·088	0·087	0·064	0·063	0·051	0·063
3	0·043	0·061	0·061	0·051	0·040	0·038	0·029	0·045
4	0·070	0·159	0·117	0·087	0·081	0·066	0·064	0·062
5	0·054	0·143	0·112	0·105	0·049	0·048	0·040	0·042
6	0·058	0·126	0·083	0·076	0·064	0·057	0·054	0·047
7	0·065	0·182	0·128	0·083	0·066	0·065	0·054	0·054
8	0·062	0·172	0·140	0·098	0·063	0·057	0·048	0·054
9	0·061	–	0·087	0·086	0·069	0·059	0·056	0·048
10	0·062	0·132	0·124	0·077	0·057	0·056	0·053	0·052
11	0·069	0·159	0·125	0·088	0·071	0·063	0·049	0·068
12	0·054	0·105	0·074	0·070	0·062	0·055	0·048	0·047
13	0·069	0·116	0·106	0·094	0·084	0·065	0·057	0·056
14	0·070	0·148	0·114	0·091	0·069	0·063	0·049	0·066
15	0·057	0·065	0·063	0·061	0·053	0·048	*	–

* Non-significant number of reflections in the interval.

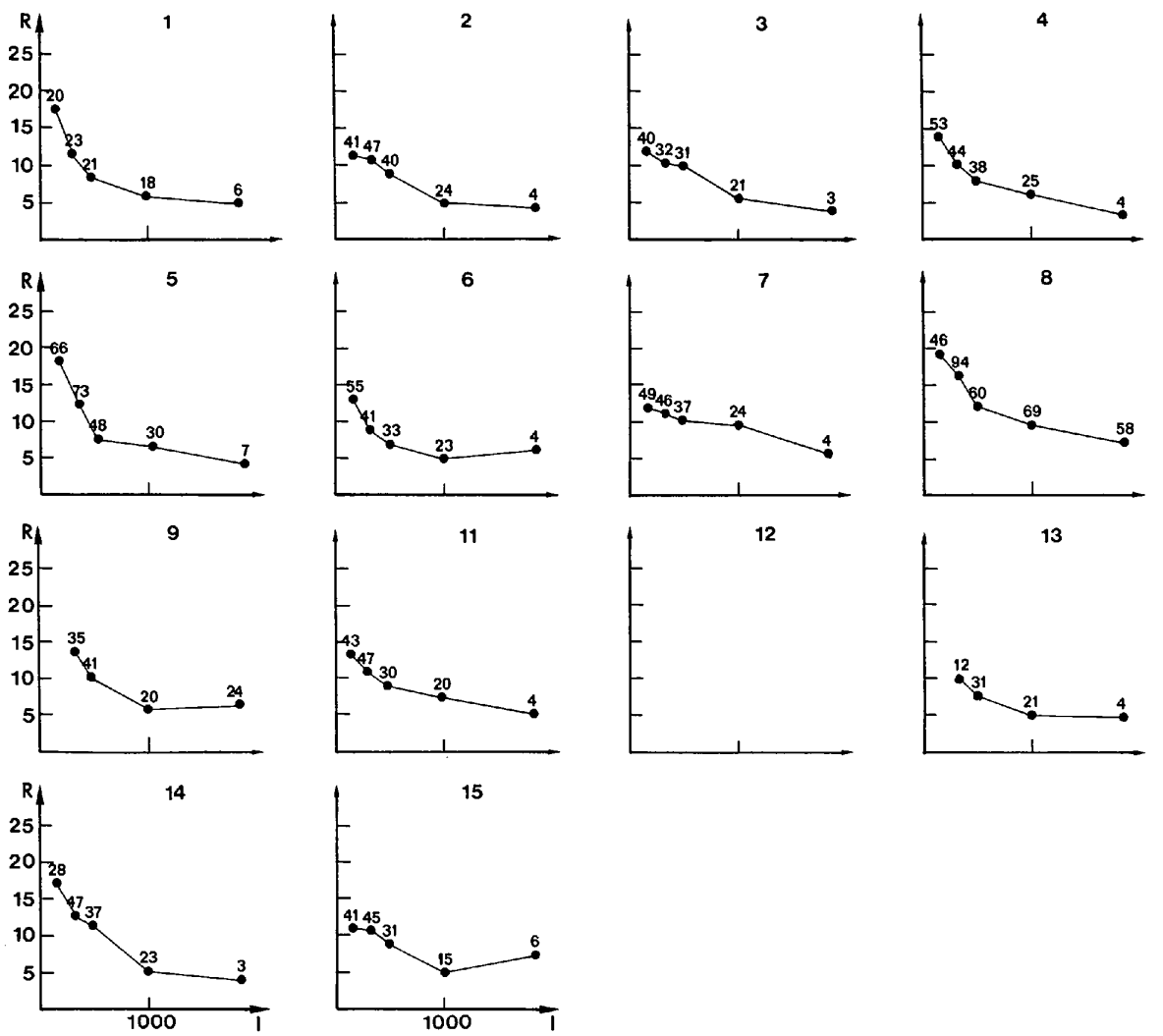

Fig. 3 R_{sym} values plotted against the intensity. All experiments from *B* film set.

By using a R_{sca} value defined as

$$R_{sca} = \sum_{hk} |I_1 - kI_2| / \tfrac{1}{2} \sum_{hk} (I_1 + kI_2), \qquad (2)$$

where k is the film factor and I_1 and I_2 are intensities from the two successive films, an analysis of the consistency between the stronger and weaker data sets may be performed. The results obtained when scaling B to A and D to C are given in Tables 10 and 11, respectively. R_{sym} values were calculated for symmetry-related reflections from the average intensity files, *i.e.* the E and F files, and the files corresponding to data sets E and F but created in our scaling procedure. For experiments 11 to 15 which use the parabolic scaling method, it has not been possible to calculate film factors, k, or R_{sca} values, since the A–D intensities are not corrected for non-linearity. The R_{sym} values were thus only obtained from the original data sets E and F.

The film factor between the B and A films varied from 2·58 to 3·20 except in two extreme cases (experiments 5 and 8 which had values of 2·13 and 1·08). For the D to C data sets the variation was 2·60 to 3·21. If the film factor for experiments 5 and 8 for scaling of B to A were excluded, average values of 2·90 and 3·00 for scaling of B to A and D to C, respectively, were obtained. The scale factors for films A and B with the smaller spots are thus systematically too low, indicating inaccuracies in the non-linearity corrections and the Wooster (1964) effect.

Mutual consistency

One measure of mutual inter-laboratory consistency for two experiments (i) and (j) is

$$R_{mut} = \sum_{hk} |I_i - I_j| / \tfrac{1}{2} \sum_{hk} |I_i + I_j|, \qquad (3)$$

where I_i and I_j are on the same scale, a mutual scale factor being refined for each R_{mut} value. Table 12 shows the R_{mut} values from set E. It is obvious that experiments 5 and 8

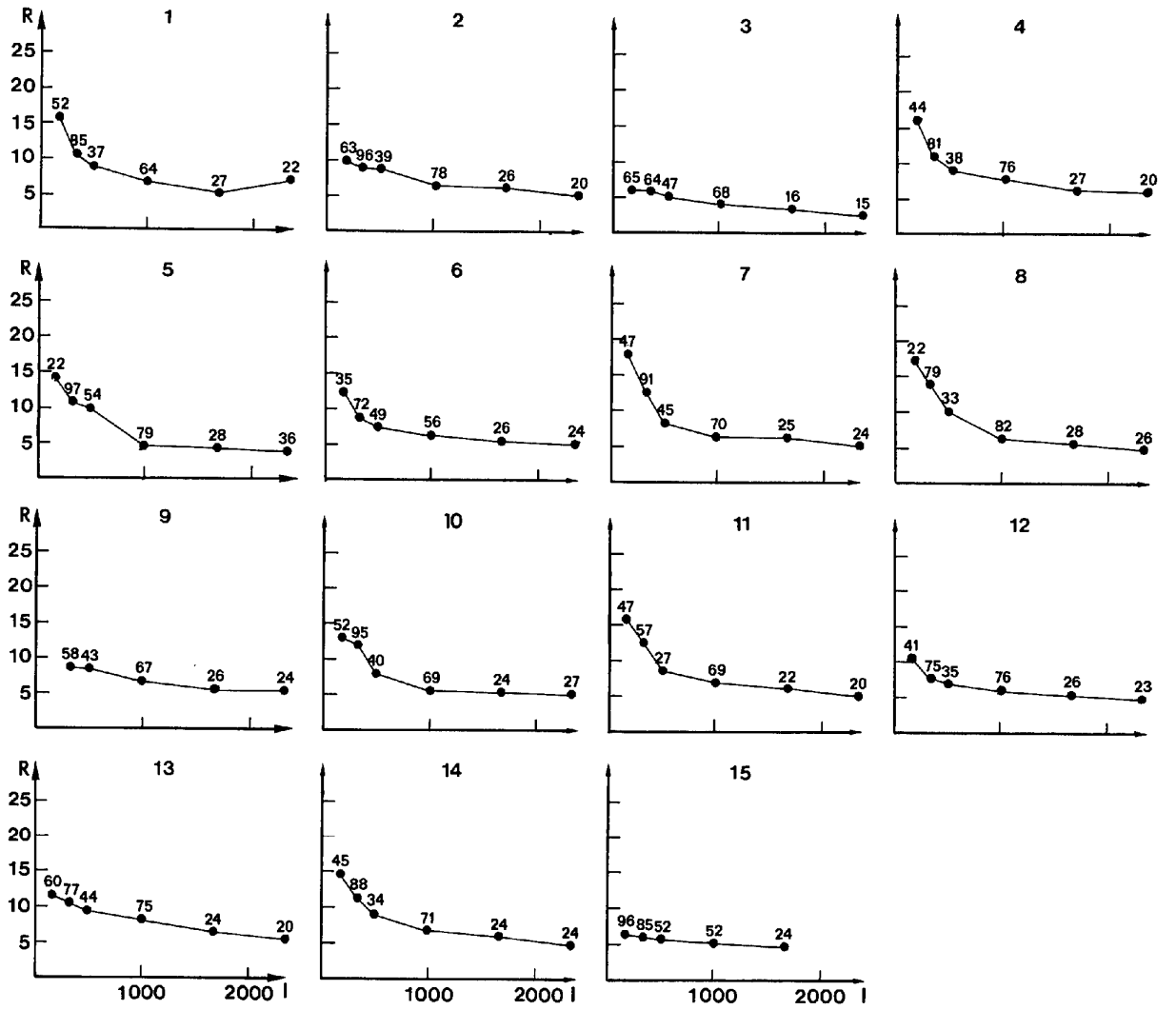

Fig. 4 R_{sym} plotted against the intensity. All experiments from C film set.

contain systematic errors, as indicated by the internal consistency test. The values of R_{mut} from the F set (Table 13) show that experiments 5, 8 and 15 differ slightly from the others.

Another way of assessing the mutual consistency is to analyse each experiment against an average value intensity file. All experiments were therefore scaled together using Hamilton, Rollett & Sparks's (1965) scaling procedure to establish two average files, one from the E and one from the F sets.

The individual intensity weights in the scaling procedure were based on $\sigma(I)$ (estimated as described previously if not given) in combination with the intensity according to

$$\sigma_{ind} = [\sigma(I)^2 + cI_i^2]^{1/2}, \quad (4)$$

where c is a constant.

In order to obtain proper weights, c was varied to give the best value for the parameter 'goodness of fit' in the program *SCALE* (*cf.* Hamilton, Rollett & Sparks, 1965). The value $c = 0{\cdot}023$ was used in the final averaging procedure and the corresponding weight analyses are given in Tables 14 and 15.

In the preparation of the final average intensity file from the E data sets, experiments 5 and 8 were rejected. The average file created from the F data sets was prepared from data from all 15 laboratories. These two average files were analysed for internal consistency, and the results are shown in Tables 16 and 17 and Fig. 8. Standard deviations for the average intensities could then be calculated from the statistical distribution of the observations, *i.e.*

$$\sigma_{av}(\bar{I}) = [\sum_i (I_i - \bar{I})^2/(N-1)]^{1/2}. \quad (5)$$

For each experiment (i), R_{av} values were also calculated, where R_{av} is defined as

$$R_{av} = \sum_{hk} |I_i - \bar{I}| / \sum \bar{I}. \quad (6)$$

I_i is an individual integrated intensity in the E or F data sets

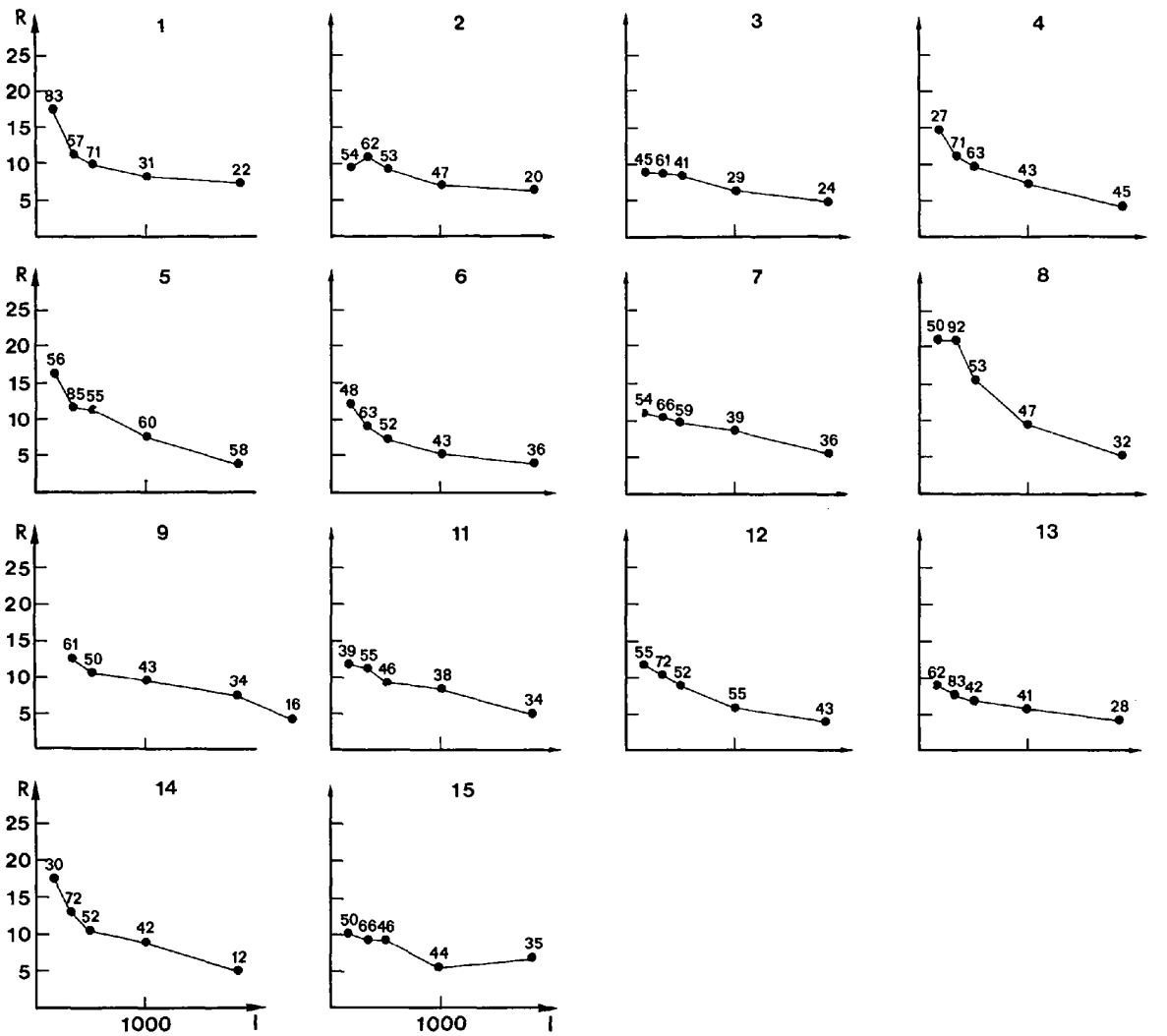

Fig. 5. R_{sym} values plotted against the intensity. All experiments from D film set.

and $\bar{I}$ is the average intensity value obtained from the scaling procedure (*cf.* Tables 14 and 15 and Figs. 9 and 10). Generally, the quantity $|I_i-\bar{I}|$ is smaller than $|I_i-I_j|$ which should be kept in mind when comparing R_{mut} and R_{av}.

Analysis of variance

The analysis of variance was performed with the program *HANOVA* (Hamilton, 1964; Abrahams, Alexander, Furnas, Hamilton, Ladell, Okaya, Young & Zalkin, 1967; Abrahams, Hamilton & Mathieson, 1970). The parameters chosen for the analysis were the experiment number n with effect $E(n)$, the intensity range I with effect $I(I)$, the angular range 2θ with effect $A(2\theta)$ and the symmetry related quadrants Q with effect $Q(q)$. The latter effect was included in order to locate errors in the positioning of the microdensitometers. Thus, the model for the analysis of variance used is

$$w_{hi}(I_{hi}-I_h)=\mu+M+EI+EA+EQ+\varepsilon, \qquad (7)$$

where I_h is the average intensity with index $hk0$, I_{hi} is the intensity of reflection $hk0$ for the ith participant, w_{hi} is a weight defined in (10) and (11), μ is the overall mean (approximately zero), M is the sum of the main effects, E, I, A and Q, EI is an experiment – intensity interaction effect, EA is an experiment – angular interaction effect, EQ is an experiment – quadrant interaction effect, and ε is a normally distributed random error.

The **F** distribution is the basis for most of the multivariate hypothesis tests and is the distribution of the ratio of two estimates of the same variance. One may assume that the weighted deviations from the average intensity,

$$X_{hi}=(I_{hi}-I_h)w_{hi}, \qquad (8)$$

has a normal random distribution for each experiment, *i.e.* that EI, EA and EQ are zero. To investigate this assumption, the **F** ratio may be calculated:

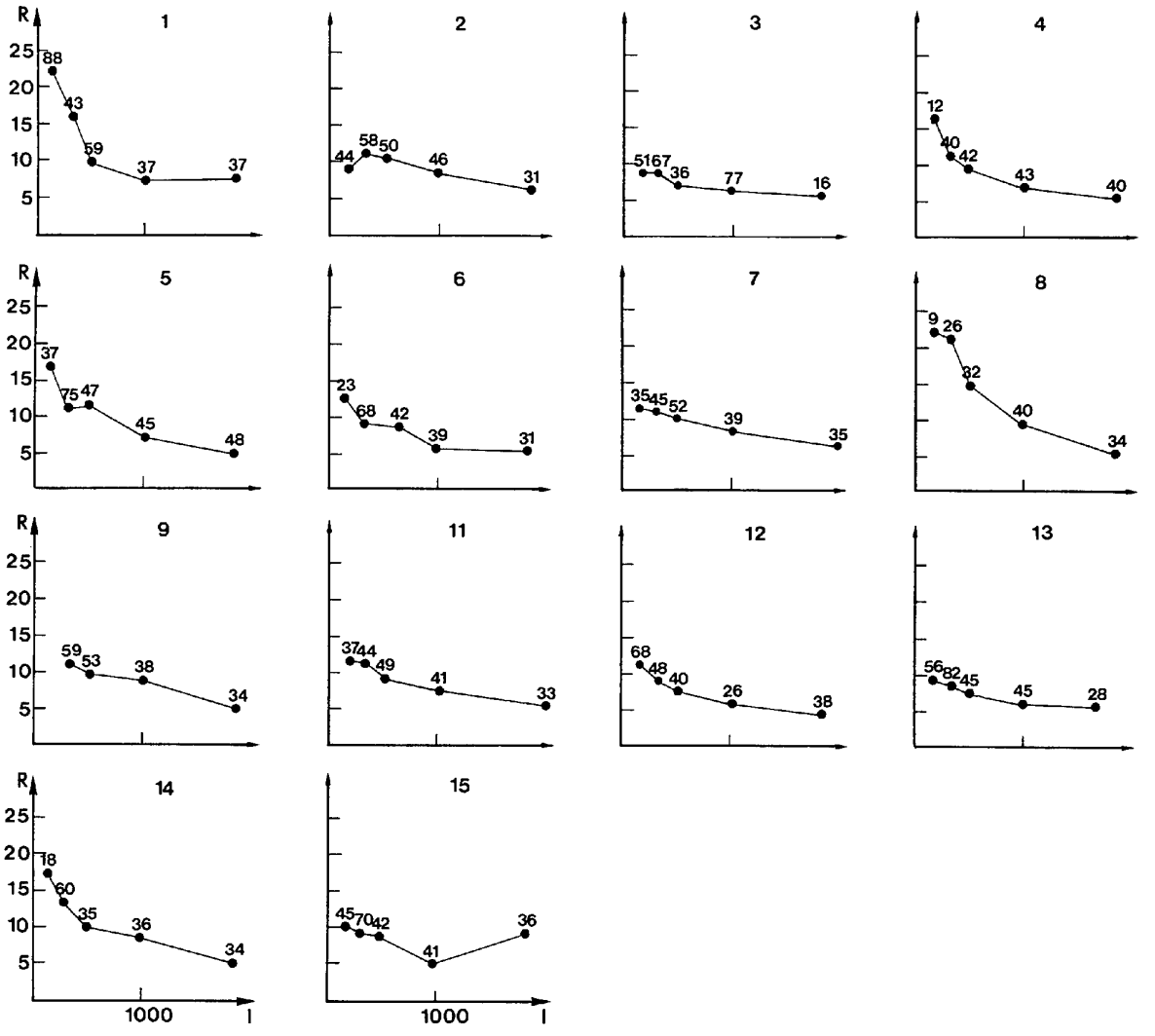

Fig. 6. R_{sym} values plotted against the intensity. All experiments from E data sets.

$$\mathbf{F}_{v_1,v_2}=[\sum_i n_i(\bar{X}'_i-\bar{X}'')^2/v_1]/[\sum_h\sum_i(X_{hi}-\bar{X}'_i)^2/v_2], \quad (9)$$

where

$$\bar{X}''=\sum_h\sum_i X_{hi}/\sum_i n_i,\ \bar{X}'_i=\sum_h X_{hi}/n_i,$$
$$v_1=k-1,\ v_2=\sum_i n_i-k$$

and n_i is the number of observations in each of the k experiments (*cf.* Larson, 1975). The **F** distribution for normal populations with the same variance has been tabulated for different degrees of freedom, v_1 and v_2, at different levels of significance, α. If the observed value of $\mathbf{F}_{v_1,v_2}$ exceeds the tabulated $\mathbf{F}_{v_1,v_2,\alpha}$ value, the variances of the compared populations are not equal at the chosen level of significance, *i.e. EI*, *EA* or *EQ* in (7) are not zero for all experiments. It is only relevant to analyse the *E* and *F* data sets, since only these sets have been corrected for non-linearity in all experiments. It is essential to introduce proper weights in (8), and two different weighting schemes have been tested:

$$w_{hi}=(I_h)^{-1}, \quad (10)$$
$$w_{hi}=(\sigma_{\mathrm{ind},hi})^{-2}, \quad (11)$$

where $\sigma_{\mathrm{ind},hi}$ is defined by (4). The use of either (10) or (11) resulted only in slightly different values of the calculated **F** ratio and did not affect the conclusions concerning the experiments. Weights according to (11) were used in the following calculations.

In the execution of the *HANOVA* program, the *E* data sets 5 and 8 were excluded, since a preliminary execution showed large *EI* and *EQ* effects for these two experiments. As the *E* data set 10 was not submitted, there are only 12 *E* data sets included in (9). Since each of the investigated interaction

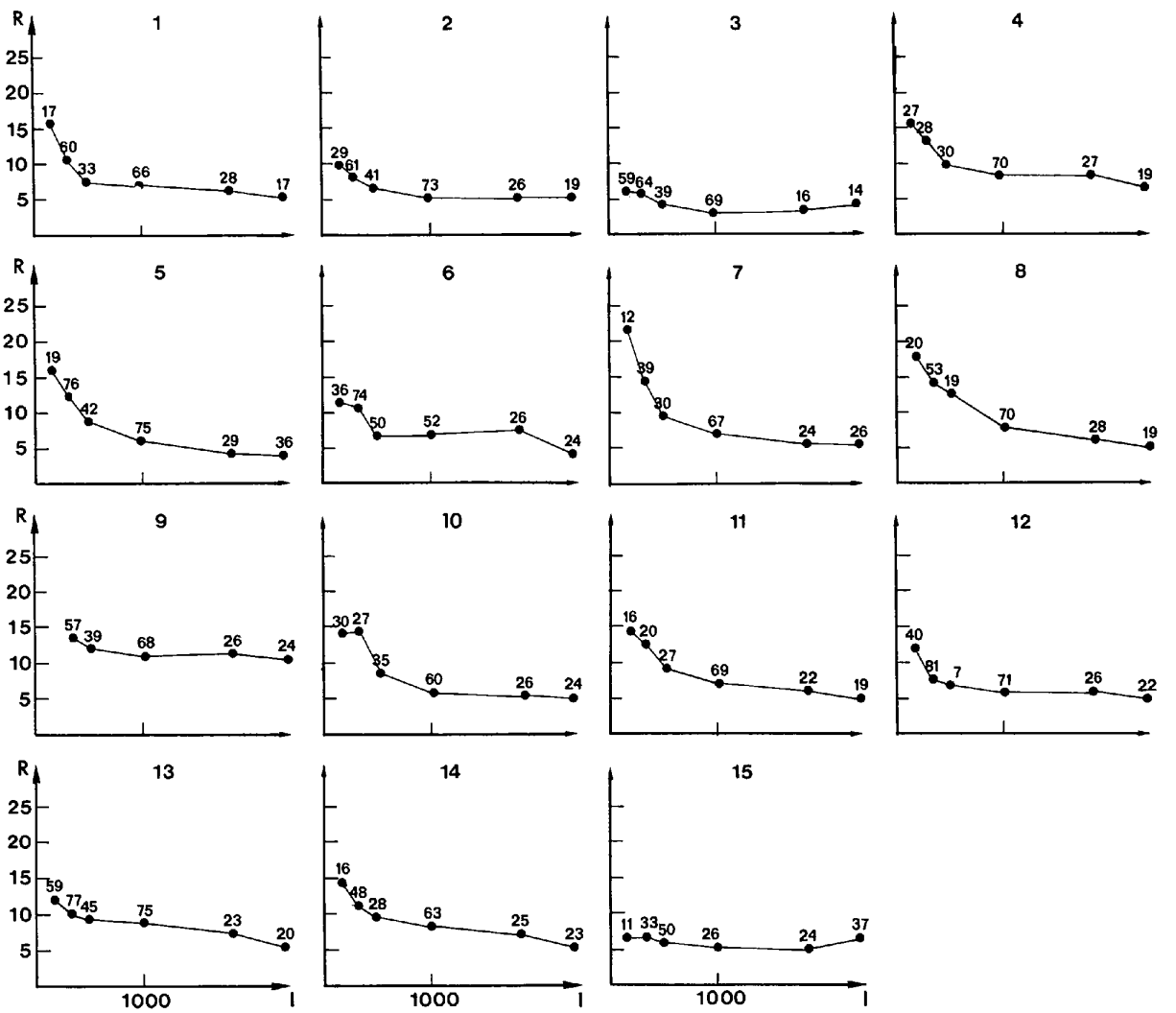

Fig. 7. R_{sym} values plotted against the intensity. All experiments from *F* data sets.

Table 10. *Agreements between symmetry-related reflections from the scaled data sets E*

The values in parentheses were obtained in our scaling procedure.

Exp. no.	R_{sca} between films	Film factor	R_{sym}	R_1	R_2	R_3	R_4	R_5	R_6	R_7
1	0·096	3·20	0·103	0·179	0·109	0·098	0·081	*	–	–
			(0·071)	(0·072)	(0·109)	(0·068)	(0·098)			
2	0·110	2·78	0·072	0·115	0·102	0·086	0·072	0·056	*	
			(0·076)	(0·142)	(0·136)	(0·083)	(0·076)	(0·055)		
3	0·064	2·95	0·066	0·088	0·085	0·082	0·063	0·062	0·054	
			(0·067)	(0·086)	(0·090)	(0·085)	(0·064)	(0·063)	(0·055)	
4	0·104	2·58	0·065	0·149	0·106	0·094	0·078	0·045	*	–
			(0·071)	(0·152)	(0·130)	(0·095)	(0·090)	(0·045)		
5	0·171	2·13	0·075	0·188	0·116	0·102	0·077	0·047	*	–
			(0·081)	(0·197)	(0·123)	(0·104)	(0·080)	(0·050)		
6	0·061	2·89	0·057	0·128	0·087	0·077	0·060	0·046	0·033	–
			(0·057)	(0·128)	(0·087)	(0·077)	(0·060)	(0·046)	(0·033)	
7	0·058	2·89	0·074	0·116	0·112	0·092	0·080	0·057	0·056	–
			(0·080)	(0·132)	(0·145)	(0·094)	(0·087)	(0·057)	(0·053)	
8	0·357	1·08	0·076	0·181	0·101	0·084	0·081	0·045	0·054	–
			(0·092)	(0·218)	(0·141)	(0·117)	(0·088)	(0·055)	(0·056)	
9	0·072	2·98	0·089	–	0·0103	0·082	0·072	0·036	0·043	–
			(0·065)		(0·104)	(0·074)	(0·092)	(0·040)	(0·046)	
10	–	–	–	–	–	–	–	–	–	–
11	–	–	0·076	0·118	0·112	0·090	0·088	0·057		–
12	–	–	0·070	0·116	0·104	0·092	0·065	0·048		–
13	–	–	0·067	0·088	0·074	0·070	0·063	0·050		–
14	–	–	0·092	0·151	0·126	0·101	0·091	0·060		–
15	–	–	0·068	0·104	0·090	0·087	0·050	0·064		–

* Non-significant number of reflections in the interval.

Table 11. *Agreement between symmetry-related reflections from the scaled data sets F*

The values in parentheses were obtained in our scaling procedure.

Exp. no.	R_{sca} between films	Film factor	R_{sym}	R_1	R_2	R_3	R_4	R_5	R_6	R_7
1	0·074	3·20	0·071	0·157	0·105	0·076	0·075	0·072	0·051	*
			(0·075)	(0·115)	(0·115)	(0·073)	(0·059)	(0·075)	(0·043)	*
2	0·061	3·21	0·056	0·100	0·084	0·069	0·057	0·051	0·045	0·055
			(0·058)	(0·093)	(0·106)	(0·071)	(0·053)	(0·058)	(0·045)	(0·055)
3	0·050	2·84	0·045	0·063	0·056	0·037	0·029	0·031	0·040	0·052
			(0·048)	(0·082)	(0·069)	(0·039)	(0·034)	(0·039)	(0·041)	(0·053)
4	0·084	3·08	0·073	0·153	0·131	0·087	0·077	0·076	0·066	0·063
			(0·074)	(0·164)	(0·140)	(0·089)	(0·075)	(0·077)	(0·072)	(0·062)
5	0·116	2·60	0·059	0·163	0·128	0·084	0·065	0·061	0·043	0·046
			(0·059)	(0·170)	(0·119)	(0·086)	(0·056)	(0·065)	(0·044)	(0·046)
6	0·058	3·12	0·061	0·117	0·110	0·065	0·074	0·075	0·044	0·052
			(0·061)	(0·117)	(0·110)	(0·065)	(0·074)	(0·075)	(0·044)	(0·052)
7	0·085	2·90	0·068	0·218	0·138	0·090	0·072	0·054	0·050	0·059
			(0·068)	(0·192)	(0·130)	(0·098)	(0·054)	(0·072)	(0·050)	(0·059)
8	0·106	2·92	0·066	0·172	0·143	0·132	0·079	0·063	0·051	0·051
			(0·073)	(0·178)	(0·151)	(0·127)	(0·065)	(0·121)	(0·051)	(0·051)
9	0·050	3·02	0·061	–	0·084	0·071	0·069	0·056	0·062	0·058
			(0·061)		(0·083)	(0·068)	(0·055)	(0·071)	(0·062)	(0·058)
10	0·068	3·13	0·065	0·141	0·147	0·080	0·055	0·057	0·053	0·058
			(0·066)	(0·143)	(0·158)	(0·084)	(0·056)	(0·057)	(0·053)	(0·058)
11	–	–	0·066	0·142	0·116	0·088	0·070	0·061	0·045	0·60
12	–	–	0·057	0·110	0·073	0·069	0·060	0·057	0·050	0·049
13	–	–	0·071	0·119	0·104	0·096	0·084	0·064	0·056	0·054
14	–	–	0·070	0·136	0·113	0·096	0·081	0·070	0·050	0·056
15	–	–	0·056	0·061	0·060	0·058	0·054	0·049	*	–

* Non-significant number of reflections in the interval.

Table 12. *Inter-experimental R_{mut} factors for E data set*

Exp. no.	1	2	3	4	5	6	7	8	9	10	11	12	13	14	15	R_{mut}	Exp. no.
1		0·106	0·110	0·103	0·296	0·109	0·116	0·224	0·107	–	0·095	0·124	0·094	0·135	0·133	0·126	1
2			0·063	0·098	0·230	0·070	0·080	0·166	0·064	–	0·075	0·085	0·071	0·094	0·091	0·093	2
3				0·096	0·212	0·048	0·078	0·142	0·064	–	0·069	0·091	0·070	0·092	0·096	0·095	3
4					0·225	0·099	0·097	0·171	0·097	-	0·117	0·079	0·075	0·095	0·086	0·111	4
5						0·247	0·208	0·266	0·231	–	0·241	0·196	0·214	0·210	0·158	0·226	5
6							0·061	0·123	0·047	–	0·070	0·116	0·080	0·088	0·114	0·098	6
7								0·112	0·055	–	0·073	0·091	0·062	0·080	0·089	0·092	7
8									0·110	–	0·151	0·237	0·146	0·168	0·201	0·171	8
9										–	0·066	0·112	0·072	0·079	0·097	0·092	9
10											–	–	–	–	–		10
11												0·126	0·085	0·094	0·119	0·106	11
12													0·080	0·094	0·080	0·116	12
13														0·089	0·086	0·094	13
14															0·100	0·109	14
15																0·112	15

Table 13. *Inter-experimental R_{mut} factors for F data set*

Exp. no.	1	2	3	4	5	6	7	8	9	10	11	12	13	14	15	R_{mut}	Exp. no.
1		0·084	0·075	0·062	0·138	0·070	0·087	0·098	0·063	0·072	0·072	0·067	0·083	0·070	0·139	0·084	1
2			0·049	0·050	0·118	0·047	0·071	0·075	0·053	0·054	0·064	0·059	0·071	0·061	0·114	0·069	2
3				0·061	0·080	0·054	0·048	0·050	0·048	0·045	0·049	0·045	0·046	0·053	0·092	0·057	3
4					0·121	0·057	0·071	0·081	0·053	0·056	0·057	0·100	0·071	0·061	0·143	0·075	4
5						0·117	0·094	0·092	0·093	0·107	0·121	0·108	0·111	0·122	0·080	0·107	5
6							0·062	0·071	0·040	0·045	0·049	0·074	0·064	0·057	0·117	0·066	6
7								0·055	0·051	0·056	0·049	0·055	0·063	0·065	0·083	0·065	7
8									0·057	0·059	0·073	0·083	0·065	0·068	0·093	0·073	8
9										0·039	0·043	0·061	0·058	0·054	0·103	0·058	9
10											0·053	0·063	0·060	0·051	0·109	0·062	10
11												0·071	0·084	0·062	0·107	0·068	11
12													0·049	0·052	0·080	0·069	12
13														0·064	0·99	0·071	13
14															0·106	0·068	14
15																0·105	15

Table 14. *Scaling of the E data sets*

Weighting scheme and R values for each experiment against the average-intensity file.

Interval no.	Total number of reflections	Average intensity	$\langle w\Delta^2 \rangle$	$R_{av,tot}$
1	1282	153	0·873	0·154
2	1138	285	1·019	0·145
3	800	508	0·925	0·098
4	694	926	1·035	0·076
5	707	1744	0·917	0·055
6	124	2652	0·864	0·089
7	21	3683	1·317	0·382

Exp. no.	R_{av}	R_1	R_2	R_3	R_4	R_5	R_6
1	0·085	0·172	0·112	0·076	0·048	0·096	
2	0·052	0·129	0·089	0·059	0·033	0·032	
3	0·047	0·101	0·070	0·046	0·039	0·036	
4	0·066	0·127	0·112	0·081	0·045	0·056	0·138
5	0·210	0·170	0·412	0·342	0·284	0·122	0·232
6	0·058	0·128	0·078	0·057	0·062	0·030	0·077
7	0·046	0·098	0·066	0·065	0·039	0·027	
8	0·184	0·238	0·319	0·170	0·093	0·052	0·090
9	0·054	-	0·100	0·057	0·039	0·029	0·074
10	–	–	–		–		
11	0·071	0·133	0·101	0·072	0·032	0·062	0·122
12	0·073	0·140	0·149	0·115	0·076	0·044	0·073
13	0·048	0·098	0·089	0·052	0·042	0·029	
14	0·065	0·170	0·125	0·071	0·050	0·026	
15	0·070	0·123	0·146	0·095	0·072	0·058	0·058

effects *EI*, *EA* and *EQ* is divided into four levels (*cf.* Table 18), the v_1 number of degrees of freedom is $12\times4-1=47$. Correspondingly, $v_2=59$ for the *F* data sets, all of which were used in the analysis. The observed $\mathbf{F}_{v_1,v_2}$ ratios, calculated according to (9), have been compared with the values tabulated on the 0·005 level of significance. If the observed

Table 15. *Scaling of the F data sets*

Weighting scheme and *R* values for each experiment against the average-intensity file.

Interval no.	Total number of reflections	Average intensity	$\langle w\Delta^2\rangle$	$R_{av,tot}$
1	1328	149	0·654	0·158
2	1369	282	1·023	0·128
3	795	533	1·003	0·080
4	1133	979	0·918	0·051
5	588	1828	0·981	0·032
6	486	3003	0·965	0·027
7	728	4627	0·880	0·040

Exp. no.	R_{av}	R_1	R_2	R_3	R_4	R_5	R_6	R_7
1	0·060	0·197	0·121	0·109	0·062	0·025	0·034	0·052
2	0·048	0·131	0·093	0·079	0·057	0·030	0·029	0·041
3	0·028	0·092	0·064	0·040	0·027	0·015	0·017	0·027
4	0·062	0·197	0·106	0·074	0·048	0·032	0·027	0·072
5	0·083	0·218	0·208	0·196	0·082	0·037	0·091	0·056
6	0·043	0·116	0·118	0·071	0·039	0·023	0·023	0·044
7	0·039	0·150	0·148	0·082	0·052	0·027	0·026	0·020
8	0·050	0·208	0·188	0·100	0·056	0·035	0·030	0·038
9	0·034	–	0·126	0·076	0·036	0·026	0·020	0·026
10	0·036	0·158	0·111	0·048	0·036	0·030	0·019	0·028
11	0·045	0·155	0·133	0·078	0·043	0·037	0·027	0·037
12	0·046	0·193	0·064	0·043	0·050	0·040	0·023	0·046
13	0·043	0·133	0·094	0·076	0·062	0·045	0·028	0·020
14	0·041	0·174	0·129	0·063	0·048	0·029	0·019	0·016
15	0·089	0·232	0·424	0·213	0·106	0·060	0·054	0·070

Table 16. *Internal consistency analysis of the average-intensity file created from the E sets*

R_{sym}	R_1	R_2	R_3	R_4	R_5	R_6	R_7
0·057	0·088	0·082	0·068	0·058	0·040	0·036	

Table 17. *Internal consistency analysis of the average-intensity file created from the F sets*

R_{sym}	R_1	R_2	R_3	R_4	R_5	R_6	R_7
0·050	0·064	0·061	0·057	0·052	0·049	0·036	0·031

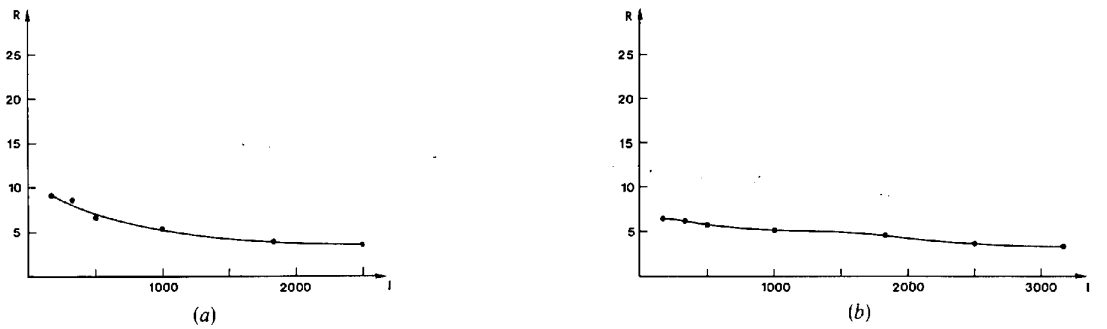

Fig. 8. (*a*) Internal consistency for the average intensity file from the *E* data sets. (*b*) Internal consistency for the average intensity file from the *F* data sets.

$\mathbf{F}_{\nu_1,\nu_2}$ ratio exceeds the tabulated $\mathbf{F}_{\nu_1,\nu_2,0.005}$ value, the hypothesis that there are no systematic differences between the experiments may be rejected. The probability of rejecting a true hypothesis is then less than 0·5 %.

Table 18. *Level intervals for the multivariate hypothesis tests*

E data sets

Variable	Level 1	Level 2	Level 3	Level 4
I	0–250	250–750	750–1500	1500–
$A(2\theta)$	0–12	12–18	18–26	26–
Q	$h>0,k>0$	$h>0,k<0$	$h<0,k>0$	$h<0,k<0$

F data sets

Variable	Level 1	Level 2	Level 3	Level 4
I	0–300	300–900	900–2000	2000–
$A(2\theta)$	0–12	12–18	18–26	26–
Q	$h>0,k>0$	$h>0,k<0$	$h<0,k>0$	$h<0,k<0$

The tabulated values for the two sets of data, *E* and *F*, are $\mathbf{F}_{47,4719,0.005}=1.67$ and $\mathbf{F}_{59,6370,0.005}=1.65$, respectively. We now assume that all data sets are identical and formulate the following hypotheses:

Hypothesis 1. The experiment–intensity interaction effects, *EI*, are zero, *i.e.* the error distributions are the same within the four intensity levels for all experiments. The calculation gave $\mathbf{F}_{47,4719}=4.81$ for the *E* data sets and $\mathbf{F}_{57,6370}=3.08$ for the *F* data sets. Thus, the above hypothesis may be strongly rejected for both sets of data. The rejection of this hypothesis means that there are systematic errors in one or more of the experiments, as was also indicated by the R_{mul} and R_{av} values.

Hypothesis 2. The experiment-angular effects, *EA*, are zero, *i.e.* there are no systematic differences between the experiments depending on the 2θ angle. The observed $\mathbf{F}_{47,4719}$ and $\mathbf{F}_{59,6370}$ values are 1·17 and 0·98 for the *E* and *F* data sets, respectively. Thus, the above hypothesis cannot be rejected either for the *E* sets nor for the *F* sets.

In the third test it was investigated whether or not there was

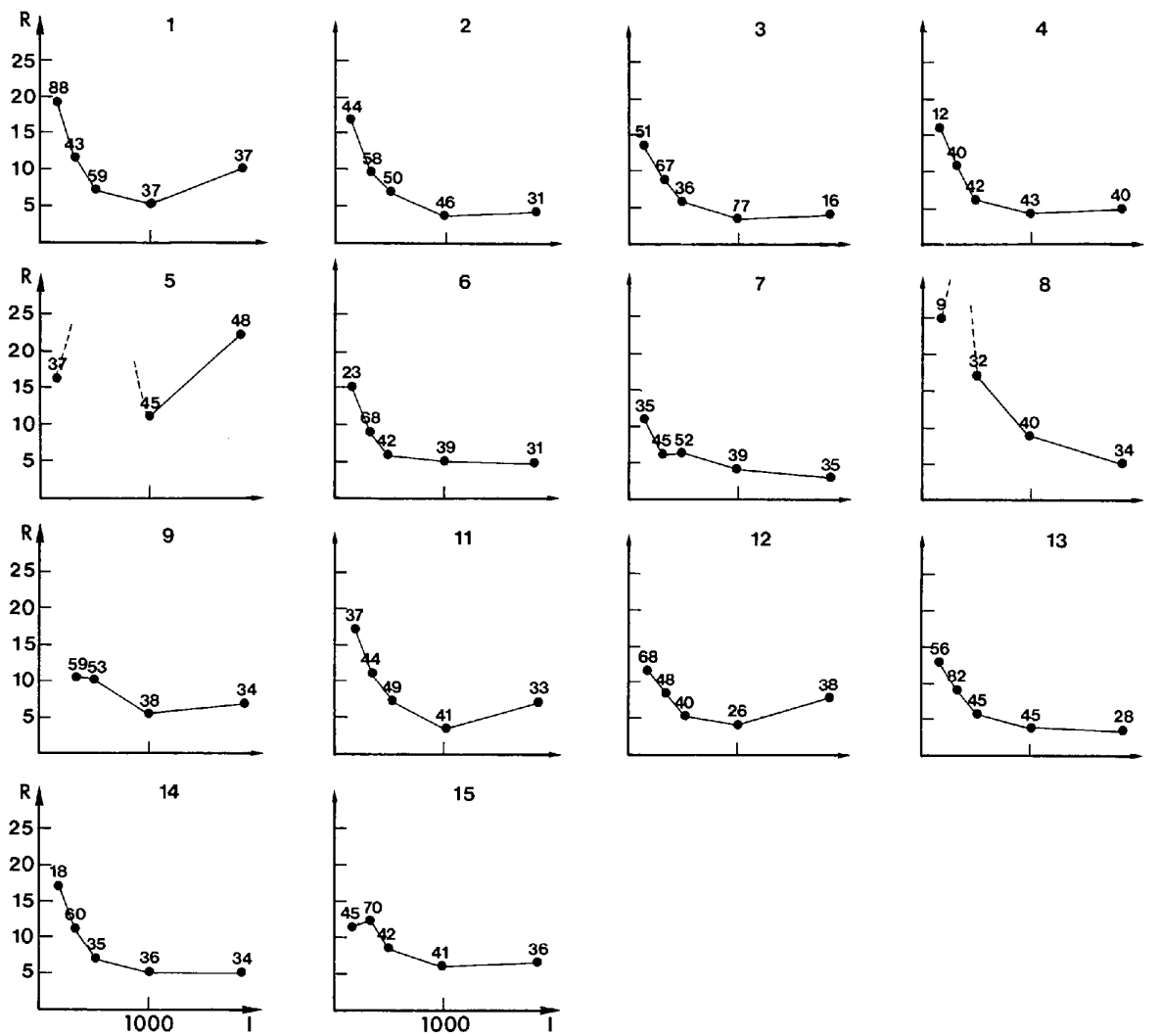

Fig. 9. Interval *R* values (R_{av}) calculated from the deviation of each experiment from the average-value file. *E* data sets.

any interaction between the experiment number and the symmetry quadrants on the films.

Hypothesis 3. Experiment–quadrant interaction effects, *EQ*, are zero, *i.e.* the error distributions are identical in the four quadrants for all experiments. The calculation gave $\mathbf{F}_{47,4719} = 3{\cdot}53$ for the *E* data sets and $\mathbf{F}_{57,6370} = 0{\cdot}94$ for the *F* data sets. The hypothesis cannot be rejected for the *F* sets as $\mathbf{F}_{57,6370,0{\cdot}005} = 1.67$ but can be rejected for the *E* data sets with a high degree of confidence. One or more experiments in the *E* set thus have systematic errors due to the scanner positioning.

The estimates of the four levels for each of the three variables *EI*, *EA* and *EQ* have been plotted explicity in Figs. 11 and 12 for each of the data sets.

Discussion

In the previous sections, the quality of each measurement has been investigated. Different *R* values, defined according to formulae (1), (2), (3) and (6), have been used to analyse the spread in the intensity measurements. Furthermore, each data set has been investigated in different intervals of intensity and angular distribution in order to examine the internal consistency of each densitometer system. These interval *R* values have been plotted against the magnitude of intensity for the different data sets *A*, *B*, *C* and *D* (in Figs. 2–5). The shapes of the curves differ from laboratory to laboratory but are often similar for the *A* and *B* data sets on one hand and for the *C* and *D* sets on the other. The data from the average intensity value files show high internal consistency, giving a good idea of the accuracy attainable with microdensitometer systems. Data from most of the participants are also homogeneous even if there are some differences in the individual results which will be commented on in this section.

General effects due to spot size

It is clearly demonstrated that the statistical spread of the intensities measured on films with small spots (*A*, *B*) is greater

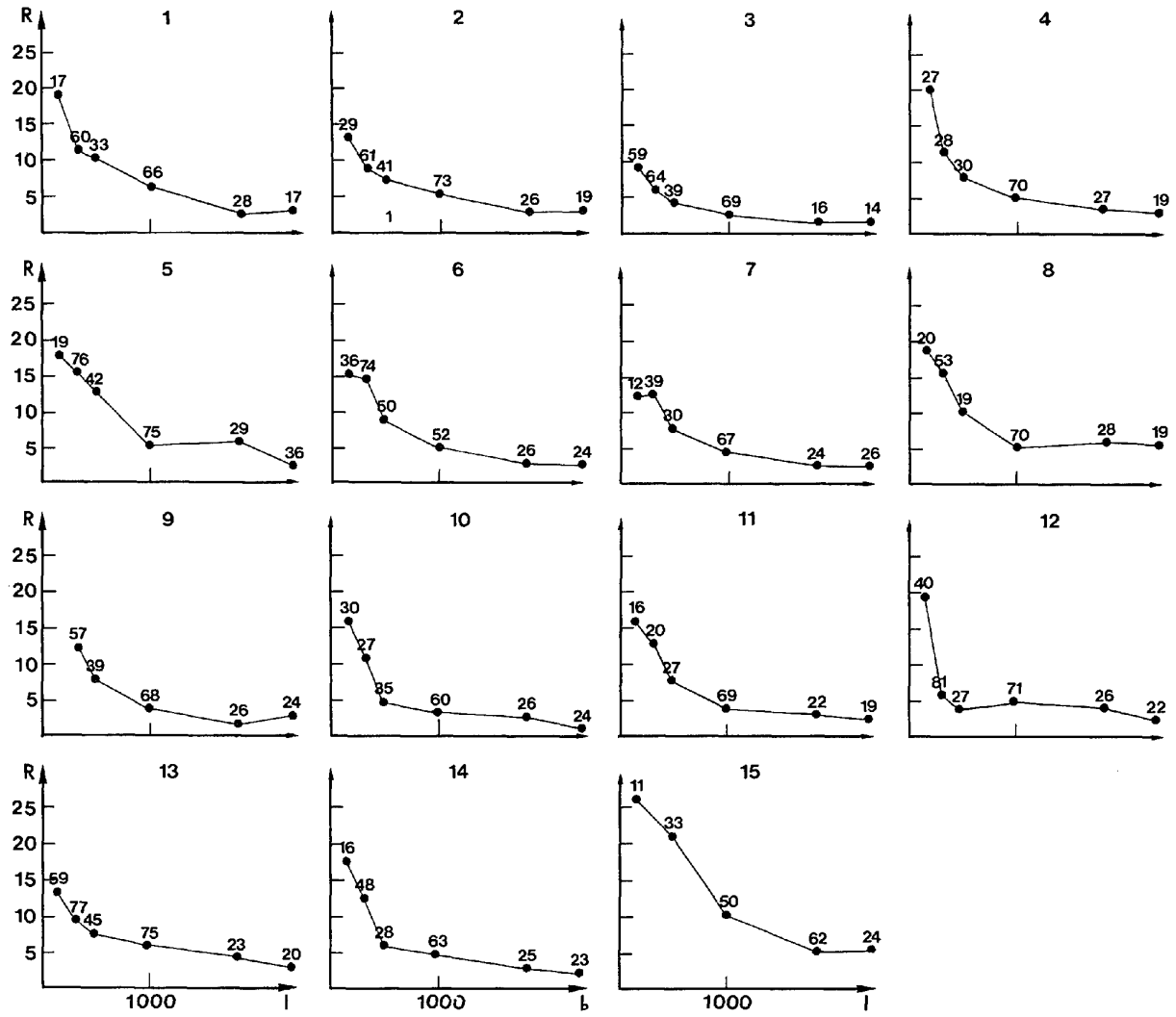

Fig. 10. Interval *R* values (R_{av}) calculated from the deviation of each experiment from the average-value file. *F* data sets.

than that obtained from films with large spots (*C*, *D*). Due to the logarithmic relationship between optical density, *D*, and the ratio of the incident to the transmitted microdensitometer light beam,

$$D = \log_{10}(I_0/I), \qquad (11)$$

it is impossible to obtain an accurate value of *D* when the blackening of the illuminated area is not uniform. This effect was pointed out by Wooster (1964) 'If the density variation across the field of view is small then the average intensity of the transmitted light will be nearly given by the average density. For a large variation of density much inaccuracy is introduced'. Fig. 13(*a*) and (*b*) shows the distribution of *R* values in different intensity intervals obtained when comparing the individual *E* and *F* data sets with the corresponding average-value files. The significant increasing trend in *R* values for strong intensities for the *E* data set (*cf.* Table 14) is not generally seen when testing the individual data sets with respect to symmetry-related reflections (Fig. 6). This effect is due to the different ways in which non-linearity corrections have been performed, together with errors due to Wooster effects. The corresponding effect for the *F* data sets is much smaller but still present (Fig. 13*b* and Table 15).

Differences between experiments: set E

The overall **F** ratios show that there are systematic differences between the data sets, regardless of whether the analysis is carried out with respect to the intensity (*EI*), angular 2θ (*EA*), or symmetry-quadrant (*EQ*) distribution. The partial **F** distributions in each level investigated are plotted and described in Fig. 11 and those experiments which

Table 19. *Deviations from the average values on the* 0·005 *significance level* (*cf.* Figs. 11 *and* 12)

E data sets

Effect	Exp. no.
EI	5, 8, 9, 11, 12, 15
EA	
EQ	1, 8

F data sets

Effect	Exp. no.
EI	5, 8, 15
EA	
EQ	5

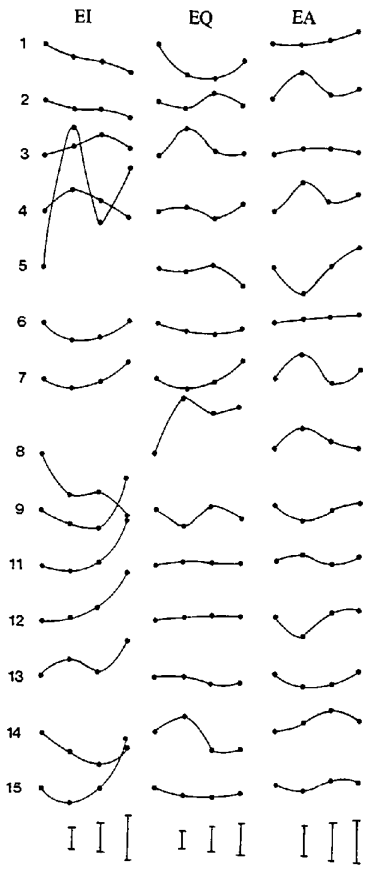

Fig. 11. Interaction effects derived by analysis of variance for the *E* data sets. There were four levels for each factor, as indicated in Table 18. Error bars 2σ in length, where σ is the estimated standard deviation of the corresponding effect as derived from th analysis of variance least-squares program, are given at the foot of the figure.

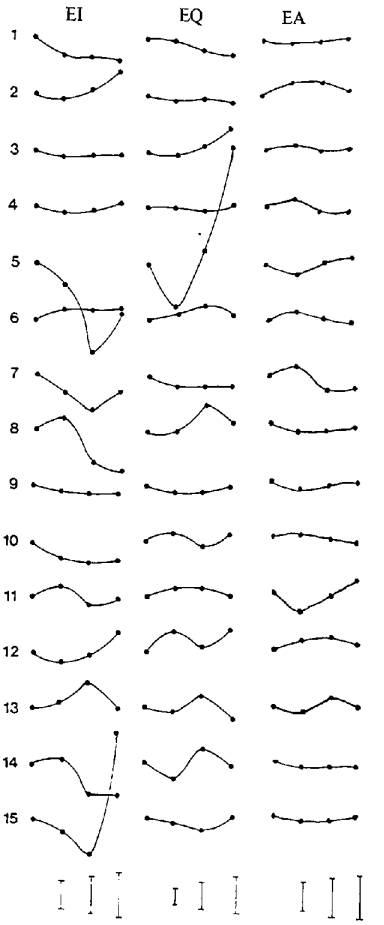

Fig. 12. Interaction effects derived by analysis of variance for the *F* data sets. There were four levels for each factor, as indicated in Table 18. Error bars 2σ in length, where σ is the estimated standard deviation of the corresponding effect as derived from the analysis of variance least-squares program, are given at the foot of the figure.

have systematic errors on the 0·005 significance level are listed in Table 19. An individual **F** ratio for each of the experiments is shown in Fig. 14.

It is apparent that experiments 5 and 8 suffer from errors which are much larger than for the other experiments in the *E* data set. This is also evident from the inter-experimental agreement factors (R_{mut}, Table 12) and the agreement with the average values (R_{av}, Table 14). When inspecting the intensity data from experiment 5 it is apparent that the weak reflections are too strong and the strong reflections too weak. It has not been possible to determine the reason for this from information available.

Experiment 8 also shows poor agreement with the other experiments. When inspecting the intensity data, reflections which should be systematically absent or very weak were found to have relatively high values, sometimes greatly exceeding $3\sigma(I)$. The overestimate was not constant, but varied considerably. It is therefore reasonable to assume that significant reflections are also biased with a varying, positive value. This is verified by a comparison with the other experiments. The error may arise from an underestimate of the background value.

Experiment 9 has been rejected with respect to *EI* effects in Table 19 since there were no reflections in the first intensity interval (*cf.* Fig. 2). The standard deviations provided by this laboratory were generally two to three times higher than the others and the weakest reflections from the first intensity interval were therefore excluded by our $3\sigma(I)$ significant test.

Experiments 11, 12 and 15 contribute most to the increasing trend of the *R* value for the strongest reflections (Fig. 13). This is also apparent from Table 14 in which the results from interval analysis of each experiment are compared with the average-value file.

It is important to note that the lower limit of transmission (*i.e.* the upper limit of measured optical density) for a relevant estimate of the optical density is dependent on the size of the reflection. Thus, an upper limit of optical density which has proved useful for large reflections may be too high for small reflections.

The high experiment–quadrant interaction shown by experiment 1 is probably accidental and due to a positioning error in the least-squares procedure for calculating the transformation matrix, since the analysis of variance test on the *C*, *D* and *F* data sets did not show the same effect. Experiment 8 also had too high an *EQ* interaction term. This could be due to an accidental mistake in the manual determination of the orientation of the film pattern.

Differences between experiments: set F

The analysis of variance tests for the *F* data sets is generally better than for the *E* sets. Fig. 12 shows plots of the four levels of the factors *EI*, *EA* and *EQ*. Experiments with significant deviations at the 0·005 level are indicated in Table 19. Again, experiments 5 and 8 are seen to differ from the average intensity file for the same reasons as in the *E* set. For experiment 15 it can be seen from Fig. 10 and Table 15 that R_{av} for the first and especially for the second intensity intervals have unexpectedly high values. Similar deviations, although not as pronounced, are found for the *E* set (*cf.* Table 14). This is probably due to a software error.

Comparison between on-line and off-line systems

From the internal and mutual consistency tests a comparison can be made between on-line and off-line systems. Experiments 5 and 8 have been rejected from the *E* set. Average *R* values for each of the on-line and off-line groups from the internal and mutual consistency tests are presented in Table 20.

Table 20. *Average R values obtained from E and F data sets for on-line and off-line systems*

	R_{sym}		R_{mut}		R_{av}	
System	*E* set	*F* set	*E* set	*F* set	*E* set	*F* set
On-line	0·077	0·064	0·091	0·070	0·048	0·064
Off-line	0·067	0·061	0·087	0·065	0·045	0·057

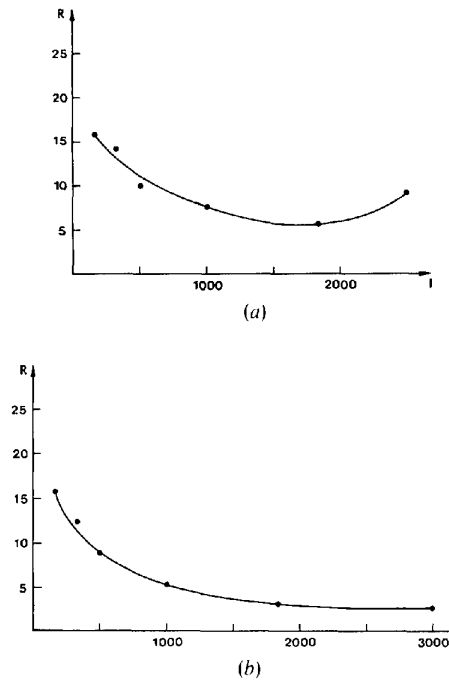

Fig. 13. The total distribution of *R* values ($R_{tot,av}$) for the *E* data sets. (*b*) The total distribution of *R* values ($R_{tot,av}$) for the *F* data sets.

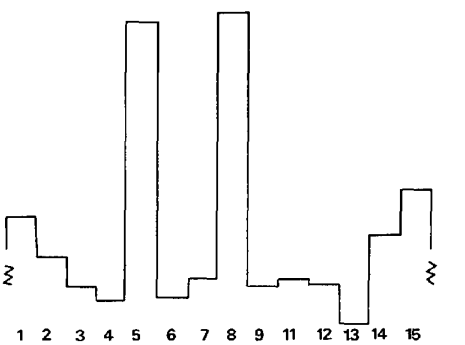

Fig. 14. Individual **F** values indicating the relative magnitudes of the systematic errors associated with the *E* data sets.

The average values of R_{sym}, R_{mut} and R_{av} for the off-line systems are all somewhat lower than those for the on-line systems. This may indicate that off-line systems yield more reliable data, since they can often utilize greater core memory and thus make use of more extensive program systems. However, if experiments 1 and 15 (both on-line systems) are excluded, since they were rejected by the program *HANOVA*, the R values for the on-line group become almost identical with those of the off-line group. Assuming that the discrepancy for experiments 1 and 15 is accidental, one may then conclude that on-line and off-line systems are equally accurate. On the other hand, experiments 1 and 15 may indeed reflect the difficulties inherent in obtaining a reliable on-line software package, especially when only a small core memory is available.

Comparison between different scaling procedures

Average R values were also calculated for the groups of participants using parabolic scaling or numerical correction of each density value (*cf.* Table 21) in order to correct for non-linearity effects, followed by linear scaling. The R values indicate that the systems which use numerical correction for each optical density are generally in better agreement than those which use the parabolic scaling procedure. The average values for R_{sym} and R_{mut} are not as useful as R_{av} in this case. R_{sym} is based on symmetry-related reflections in the four quadrants, and is not affected by errors in the correction for non-linearity. Neither are the average values of R_{mut}, as given in Tables 12 and 13, useful. A new set of R_{mut} values was calculated separately for the two groups; parabolic or numerical, respectively. Then it became evident, as can be seen in Table 22, that the accuracy is better for users of numerical non-linear correction followed by linear scaling of the two films.

Table 21. *Average R values from E and F sets for the two groups parabolic scaling (exp. nos. 10–15) and linear scaling (exp. nos. 1–9) after numerical non-linearity correction*

	R_{sym}		R_{mut}		R_{av}	
System	*E* set	*F* set	*E* set	*F* set	*E* set	*F* set
Parabolic	0·075	0·064	0·091	0·075	0·065	0·053
Linear	0·071	0·062	0·088	0·064	0·058	0·044

Table 22. *Modified average R'_{mut} values, calculated separately, for the groups of parabolic and linear scaling*

	R'_{mut}	
System	*E* set	*F* set
Parabolic	0·095	0·077
Linear	0·084	0·058

The parabolic scaling procedure should not be used on films with different spot sizes (*e.g.* Weissenberg films and oscillation films). If, however, films with constant spot sizes are scanned, the parabolic scaling procedure, properly weighted, may have advantages in minimizing Wooster effects.

The average microdensitometer data

In the analysis of the individual E and F data sets, we have found a concordant group of experiments with a relatively good internal homogeneity. By using this data, average intensity files have been created.

As stated previously, only experiments 5 and 8 were rejected from the E data set, even though the analysis of variance indicated that other experiments from both sets were affected by systematic errors. On the other hand, an **F** ratio calculation on the 0·005 significance level is a very sensitive test and deletion of more experiments could lead to successive rejections. The two average-value files from each data set E and F have been analysed as being separate experiments. The results from the internal consistency test on the two files is shown in Tables 12 and 13 and Fig. 9. The R_{sym} values obtained from the two files (0·057 and 0·050 for E and F, respectively) appear to be satisfactory. Both crystals used in this project gave R_{sym} values of 0·050 for corresponding $hk0$ reflections measured with a Syntex $P2_1$ diffractometer. Further comparison with diffractometer data will be given in Report II.

The agreement between the weak reflections is generally better for the average files than for any of the individual experiments, which is to be expected if the errors are mainly randomly distributed.

Size of light beam

It has been seen that films with small spot sizes give worse agreement than those with large spot sizes, due to the Wooster effect (*cf.* Tables 10 and 11). Normally, all films were measured with a light-beam size of 100×100 μm, but two participants, 6 and 7, used a raster size of 50×50 μm for the A/B film set. The results in Table 14 may indicate an improvement when the raster size is lowered to 50 μm for the small spots. However, the F data sets 6 and 7 are also of good quality (Table 15) and it is not therefore possible to draw any definite conclusions.

Choice of radiation and film

The principal difference between film and diffractometer methods is that films suffer from unfavourable build-up of background during data collection (Arndt, 1968). For this reason, it is advisable to use monochromatized radiation in order to reduce the background as much as possible.

The choice of film is also of great importance. In this project Ilford Industrial G film, which was recommended by Morimoto & Uyeda (1963), has been used. Unfortunately, this film is no longer manufactured. However, since the film quality is not one of the parameters of this project, it has no bearing on the present results. Another IUCr Commission on Crystallographic Apparatus project is investigating characteristics of X-ray films now available.

Choice of microdensitometer and computer systems

As the main group of participants (12) in this project use an Optronics drum microdensitometer it is not possible to compare different types of scanners. There would seem to be no distinct difference in quality between on-line and off-line systems, and the choice between one or the other may therefore be dictated by the local situation.

Evaluation of standard deviations

There are many different ways of evaluating the standard deviations, but two procedures dominate within this project, *i.e.* a quantum statistical expression (*cf.* experiments 3, 9, 14) and a scanner optics expression (*cf.* experiments 2, 6, 7). However, none of the estimates of a standard deviation of an intensity measurement, based on either of these two procedures reproduce the variation in intensity found in

practice. We have calculated the statistical standard deviation, defined as

$$\sigma_{\text{stat}} = [\sum_{i}^{n} (I_i - \bar{I})^2/(n-1)]^{1/2}, \quad (12)$$

where $\bar{I}$ is the average intensity, I_i is the scaled intensity value for the ith participant and n is the number of participants contributing to the average intensity value. The values of σ_{stat}/I have been estimated and averaged in different intensity intervals (*cf.* Fig. 15).

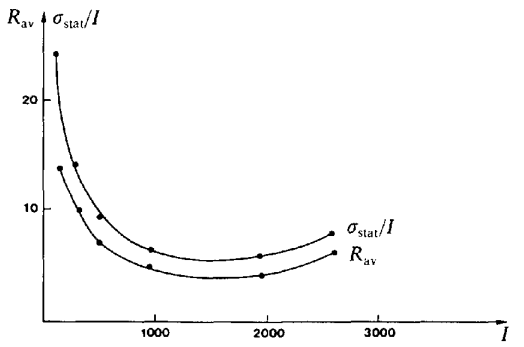

Fig. 15. The factors σ_{stat}/I and interval R_{av} plotted against the intensity.

Neither the quantum-statistics-related nor the scanner-optics-related standard-deviation expressions describe the curves found in Fig. 15, and especially the rising trend for the E data sets cannot be achieved. A reasonable calculation of $\sigma(I)$ values may instead be based on a combination of the two different procedures, since they describe two independent effects. In addition, a third empirical term should be included to compensate for systematic errors such as Wooster effects.

We wish to thank Dr Susan Jagner for many valuable comments and revision of the English text.

References

ABRAHAMS, S. C., ALEXANDER, L. E., FURNAS, T. C., HAMILTON, W. C., LADELL, J., OKAYA, Y., YOUNG, R. A. & ZALKIN, A. (1967). *Acta Cryst.* **22**, 1–6.

ABRAHAMS, S. C., HAMILTON, W. C. & MATHIESON, A. MCL. (1970). *Acta Cryst.* A**26**, 1–18.

AMBADY, G. K. & KARTHA, G. (1968). *Acta Cryst.* B**24**, 71–83.

ARNDT, U.W. (1968). *Acta Cryst.* B**24**,1355–1357.

HAMILTON, W. C. (1964). *Statistics in Physical Science*. New York: Ronald Press.

HAMILTON, W. C., ROLLETT, J. S. & SPARKS, R. A. (1965). *Acta Cryst.* **18**, 129.

LARSON, H. J. (1975). *Statistics: An Introduction*. New York: John Wiley & Sons.

MORIMOTO, H. & UYEDA, R. (1963). *Acta Cryst.* **16**, 1107–1119.

WOOSTER, W. A. (1964). *Acta Cryst.* **17**, 878–882.